

Electronic Effects in Asymmetric Catalysis: Structural Studies of Precatalysts and Intermediates in Rh-Catalyzed Hydrogenation of Dimethyl Itaconate and Acetamidocinnamic Acid Derivatives Using C_2 -Symmetric Diarylphosphinite Ligands

T. V. RajanBabu,* Branko Radetich, Kamfia K. You,[†] Timothy A. Ayers,[‡]
Albert L. Casalnuovo,[§] and Joseph C. Calabrese[⊥]

Department of Chemistry, The Ohio State University, Columbus, Ohio 43210, and DuPont Central Research and Development, Experimental Station, Wilmington, Delaware 19880

Received January 22, 1999

Enantioselectivity of Rh(I)-catalyzed asymmetric hydrogenation of dehydroamino acid derivatives and dimethyl itaconate can be enhanced by the appropriate choice of substituents on the aromatic rings of vicinal diarylphosphinites derived from carbohydrates as well as *trans*-cyclohexane-1,2-diol. For example, the use of phosphinites with electron-donating bis(3,5-dimethylphenyl) groups at phosphorus provide high ee's in these reactions whereas electron-withdrawing aryl substituents decrease the enantioselectivity. In this paper, an attempt is made to clarify the origin of these remarkable electronic effects at two levels. First, crystal structures of a number of precatalysts ($[\text{phosphinite}]_2\text{Rh}^+[\text{diolefin}]\text{X}^-$) were determined and their structures were studied in detail to examine the electronic effects, if any, on the ground-state conformations of these molecules. A study of six of these complexes reveals that the gross conformational features of these precatalysts are largely unaffected by electronic effects, which suggests that other explanations have to be sought for the electronic amplification of enantioselectivity. One possibility is a change in the diastereomeric equilibrium between the initially formed $[\text{substrate}]\text{Rh}^+[\text{phosphinite}]$ complexes as a function of electronic effect of the ligand. In the Rh-catalyzed hydrogenation of dimethyl itaconate, we have examined this equilibrium between the major and minor complexes by ^{31}P NMR. There is a clear difference in the ratio of these two diastereomers when 3,5-dimethylphenylphosphinite vis-à-vis the unsubstituted diphenylphosphinite is used. Electron-deficient ligands such as 1,2-bis-3,5-difluorophenylphosphinite and 1,2-bis-3,5-bis-trifluoromethylphenylphosphinite appear to form these diastereomers more readily at room temperature, even though the exact ratio of the diastereomers could not be established with any certainty.

Introduction

Strategies for controlling the regio- and stereoselectivity of reactions is at the heart of modern organic chemistry research. In asymmetric catalysis using organometallic reagents, where the origin of selectivity depends on the properties of a chiral ligand, two principal levels of induction can be recognized.¹ (a) Catalyst–substrate interactions lead to diastereomeric intermediates of widely different thermodynamic stabilities, each reacting at comparable rates (or the more stable diastereomer reacting faster), resulting in a reaction whose selectivity can be predicted with reasonable certainty if the diastereomeric composition is known. In this case, if the exact structure of the major diastereomer can be deduced, for example, from X-ray crystallography or from solution NMR studies, there is also the possibility of tuning the ligand to maximize the enantioselectivity.^{2,3} (b) A second limiting scenario is when the reactivities

rather than the thermodynamic stabilities of the diastereomeric intermediates play a major role. In these instances, it is impossible to predict, even qualitatively, the selectivity of the reaction without knowing the details of the kinetics and the position of the equilibrium involving the relevant diastereomeric intermediates. In most cases, a combination of both of these factors operates. As in the case of the well-studied Rh-catalyzed hydrogenation of acetamidoacrylic acid derivatives,⁴ the reaction could be under Curtin–Hammett conditions and the structure of

[†] Current address: BASF Corp., 1609 Biddle Ave., Wyandotte, MI 48192.

[‡] Current address: Hoechst Marion Roussel, 2110 East Galbraith Rd, Cincinnati, OH 45215.

[§] Current address: DuPont Agricultural Products, Stine-Haskell Research Center S300/124, Newark, DE 19714.

[⊥] Questions regarding X-ray structures should be addressed to J.C.C. at DuPont Central Research.

(1) (a) Bosnich, B. *Asymmetric Catalysis*; Martinus Nijhoff Publishers: Dordrecht, 1986. (b) For a recent incisive analysis, see: Heller, D.; Buschmann, H. *Top. Catal.* **1998**, *5*, 159.

(2) For some recent examples, see: (a) Trost, B. M.; Van Vranken, D. L. *Chem. Rev.* **1996**, *96*, 395 and references therein. (b) Bao, J.; Wulff, W. D.; Rheingold, A. L. *J. Am. Chem. Soc.* **1993**, *115*, 3814. (c) Corey, E. J.; Noe, M. C. *J. Am. Chem. Soc.* **1993**, *115*, 12579.

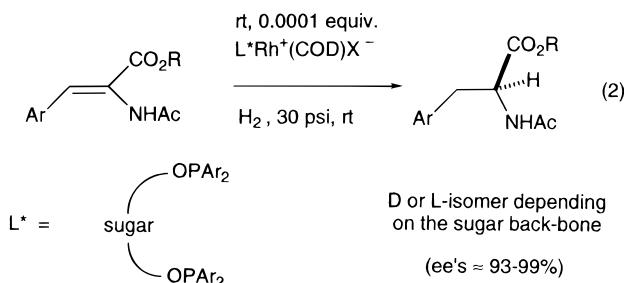
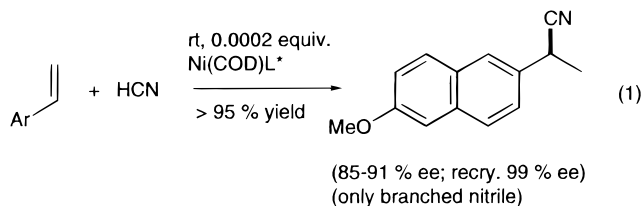
(3) Pd-catalyzed allylation of stabilized nucleophiles provides one of the best examples of the use of structural information of diastereomeric complexes in the design of a catalyst. For selected recent references, see: (a) Trost, B. M.; Van Vranken, D. L.; Bingel, C. *J. Am. Chem. Soc.* **1992**, *114*, 9327. (b) Allen, J. V.; Coote, S. J.; Dawson, G. J.; Frost, C. G.; Martin, C. J.; Williams, J. M. J. *J. Chem. Soc., Perkin Trans. 1* **1994**, 2065. (c) Sprinz, J.; Kiefer, M.; Helmchen, G.; Reggelin, M.; Huttner, G.; Walter, O.; Zsolnai, L. *Tetrahedron Lett.* **1994**, *35*, 1523. (d) Brown, J. M.; Hulmes, D. I.; Guiry, P. J. *Tetrahedron* **1994**, *50*, 4493. (e) Togni, A.; Breutel, C.; Snyder, A.; Spindler, F.; Landert, H.; Tijani, A. *J. Am. Chem. Soc.* **1994**, *116*, 4062. (f) von Matt, P.; Lloyd-Jones, G. C.; Minidis, A. B. E.; Pfaltz, A.; Macko, L.; Neuburger, M.; Zehnder, M.; Rüegger, H.; Pregosin, P. S. *Helv. Chim. Acta* **1995**, *78*, 265. (g) Seebach, D.; Devaquet, E.; Ernst, A.; Hayakawa, M.; Kühnle, F. N. M.; Schweizer, W. B.; Weber, B. *Helv. Chim. Acta* **1995**, *78*, 1636. (h) Peña-Cabrera, E.; Norrby, P.-O.; Sjögren, M.; Vitagliano, A.; De Felice, V.; Oslob, J.; Ishii, S.; O'Neill, D.; Akermark, B.; Helquist, P. *J. Am. Chem. Soc.* **1996**, *118*, 4299.

Table 1. Electronic Effects in Asymmetric Catalysis^a

Entry	L* =	Enantioselectivity (%ee) at rt	
		Hydrocyanation (eq 1)	Hydrogenation (eq 2)
1.	9a	16	99
2.	9b	33	94
3.	9d	78	71
4.	9e	85 (91 at 0 °C)	60

^a For a more complete list see refs 5b and 6b.

the catalytically relevant diastereomer may not be known with any certainty. To obtain high selectivities from such reactions, an empirical approach to ligand design remains a powerful option. In our previous work on the enantioselective hydrocyanation (eq 1)⁵ and hydrogenation (eq 2) reactions,⁶ we have shown that the selectivity and



efficiency of a catalyst system can be optimized by the choice of a tunable ligand system whose steric and electronic properties can be systematically varied, whether the effects of such variations are predictable. As shown in Table 1, one of the important outcomes of these early studies was the emergence of electronic effects of ligands as a control element in asymmetric catalysis.⁷ Using sugar phosphinites (L*) as ligands, we have shown that in the Ni(0)-catalyzed asymmetric hydrocyanation of vinyl arenes electron-deficient ligands enhance the enan-

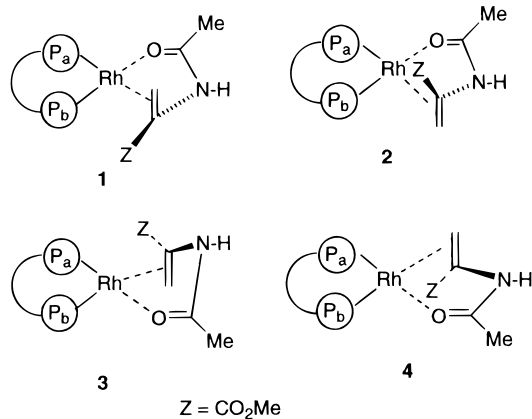


Figure 1. Diastereomeric P₂Rh(I) complexes of acetamidoacrylates. When the ligand is C₂-symmetric, **1** and **3** (also **2** and **4**) are identical.

tiostereoselectivity, whereas in Rh(I)-catalyzed hydrogenation, electron-rich phosphinites are the most ideal.

While the sugar-derived phosphinites are among the most easily accessible ligands, and their use results in the *highest* enantioselectivities for the hydrogenation and hydrocyanation reactions for several substrates, the non-C₂-symmetric nature of the backbone leaves several unanswered questions about the role of the unsymmetrical backbone. For example, consider the potential intermediates **1**–**4** shown in Figure 1. In a truly C₂-symmetric ligand there will be only two square-planar Rh(I) complexes: **1** will be equivalent to **3**, and **2** will be equivalent to **4**. But the unsymmetrical backbone of **9** (or **10**) breaks such symmetry, making **1** and **3** marginally different in these cases, even though both lead to addition of H₂ from the *Si* face of the prochiral olefin. The role of each of these intermediates was not obvious from our previous studies. For example, the reactivities of **1** and **3** could be different in the subsequent rate-determining oxidative addition to form the octahedral Rh(III) hydride. This difference would have an effect on the selectivity, which may be superimposed on the electronic effects we observed. To eliminate the potential contributions to selectivity by such intermediates and truly gauge the electronic effects in the absence of any other ligand biases, we undertook a study of the hydrogenation of acetamidocinnamic acid derivatives using truly C₂-symmetric diarylphosphinites from optically pure *trans*-1,2-cyclohexanediol. The results of these studies are reported in this paper. Having experimentally confirmed the electronic effects in this C₂-symmetric system, we decided to examine the ground-state conformations of several precatalysts [(L)Rh(I)(di-olefin)]⁺X⁻ by X-ray crystallography. In the case of C₂-symmetric (and a few non-C₂-symmetric) ligands that form five- and seven-membered Rh-chelates, some degree of success has been achieved in relating the conformation of the precatalyst to the sense of asymmetric induction (*vide infra*, ref 27). Thus, the first question is, can electronic effect of a ligand alone bring about a conformational change in the precatalyst? If so, does this fit the already established empirical relationships?

Two other important questions related to the origin of electronic amplification of enantioselectivity in the Rh-catalyzed asymmetric hydrogenation are as follows: (i) How are the relative reactivities of the two diastereomers affected by ligand electronics? (ii) What is the effect of

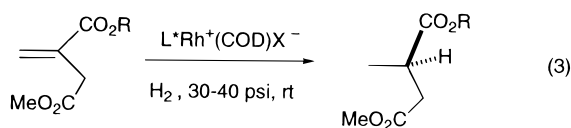
(4) (a) Landis, C. R.; Halpern, J. *J. Am. Chem. Soc.* **1987**, *109*, 1746. (b) Brown, J. M. *Chem. Soc. Rev.* **1993**, *25*. (c) Bircher, H.; Bender, B. R.; von Philipsborn, W. *J. Magn. Reson. Chem.* **1993**, *31*, 293.

(5) (a) RajanBabu, T. V.; Casalnuovo, A. L. *J. Am. Chem. Soc.* **1992**, *114*, 6265. (b) Casalnuovo, A. L.; RajanBabu, T. V.; Ayers, T. A.; Warren, T. H. *J. Am. Chem. Soc.* **1994**, *116*, 9869.

(6) (a) RajanBabu, T. V.; Ayers, T. A.; Casalnuovo, A. L. *J. Am. Chem. Soc.* **1994**, *116*, 4101. (b) RajanBabu, T. V.; Ayers, T. A.; Halliday, G. A.; You, K. K.; Calabrese, J. C. *J. Org. Chem.* **1997**, *62*, 6012.

(7) Several leading references to the role of electronic effect as a control element in asymmetric catalysis can be found in refs 5 and 6. For a more recent report, see: Palucki, M.; Finney, N. S.; Pospisil, P. J.; Güller, M. L.; Ishida, T.; Jacobsen, E. N. *J. Am. Chem. Soc.* **1998**, *120*, 948.

ligand electronics on the ratio of the major and minor diastereomers? Of these effects, the former is more intractable.⁸ However, the effect of ligand electronics on the ratio of the major to minor diastereomers, in principle, is more discernible, especially in the Rh-catalyzed hydrogenation of dimethyl itaconate^{13,14} (eq 3), a reaction

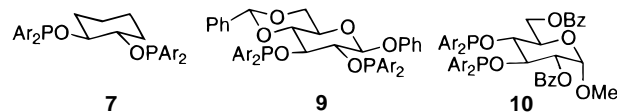
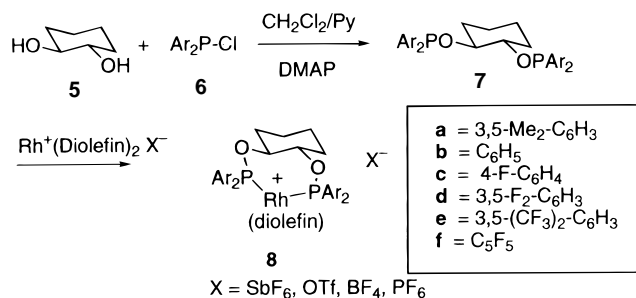


that shares important mechanistic similarities with the acetamidoacrylate reductions. In the itaconate system, the diastereomeric intermediates can be more easily characterized by low-temperature NMR spectroscopy.¹³ Here we report our attempts to probe the ligand electronic effects on the equilibrium between the major and minor diastereomers. An added impetus for the study of itaconate hydrogenation is the importance of succininc acid derivatives as valuable intermediates for several pharmaceutical preparations including potent renin inhibitors.¹⁵ The results of these studies are also reported in this paper.

Results and Discussion

Synthesis of the C₂-Symmetric Ligands and Their Complexes: *trans*-1,2-Diarylphosphinoxycyclohexane. (*S,S*)-(+)-*trans*-1,2-bis(diphenylphosphinoxy)cyclohexane was one of the first phosphinites used in Rh-catalyzed asymmetric hydrogenations.¹⁶ The enantiomeric purity of the ligand and, therefore, the enantioselectivity

Scheme 1. Synthesis of 1,2-Diarylphosphinoxycyclohexane



of the reactions in which they were used were low. We prepared both the (+) and the (-) ligands from commercially available 1,2-cyclohexanediols (99% ee) and the corresponding diarylchlorophosphines^{5b} by procedures reported previously (Scheme 1).¹⁷ Likewise, the cationic Rh-complexes were prepared by reacting stoichiometric amounts of Rh⁺(diolefin)₂X⁻ [diolefin = norbornadiene, 1,4-cyclooctadiene; X = OTf, SbF₆, or BF₄] and the diarylphosphinite in methylene chloride, acetone, or THF.¹⁸ These compounds were fully characterized by ¹H and ³¹P NMR and in selected cases (vide infra) by X-ray crystal structure determination. The ³¹P NMR of the ligands and the complexes are recorded in Table 2.

Hydrogenation of Dimethyl Itaconate. The hydrogenation of dimethyl itaconate using various cationic Rh-complexes were carried out at 30–40 psi of hydrogen in a Fischer–Porter tube. The results of hydrogenation using complexes of **7a–e** are shown in Table 3. For comparison, the results of the reductions with two C₁ symmetric ligands derived from carbohydrates⁶ (**9** and **10**) are also included in Table 3. In each case, the enantiomeric excess was determined by chiral GC on a Chiraldex GTA column. The absolute configuration of the product was assigned on the basis of a comparison of elution properties of an authentic sample prepared by hydrogenation of dimethyl itaconate using (2*S*,4*S*)-BPPM-(Rh⁺)(COD) SbF₆⁻ catalyst, which is known to produce predominantly the (*S*)-isomer.¹⁵ As can be seen from Table 3, the enantioselectivity depends on the electronic nature of the *P*-Ar substituent, with the electron-deficient phosphinites giving poor selectivity. As the electron density of the aromatic ring, and presumably that on Rh, is reduced the ee falls off precipitously. The Σσ values, which are a measure of the combined electronic effect of the groups, parallel the enantioselectivity of the reaction in each case. The case of the *p*- vs *m*-fluorine substituent is particularly interesting. The σ value for the *p*-F substituent is 0.06 while that for *m*-fluoro substituent is 0.34, clearly showing the diminished electron-withdrawing effect of a fluorine in the para position, presumably due to the resonance-donating effect.¹⁹ From a synthetic

(8) The origin of the difference in the reactivities of the two diastereomeric Rh(I) complexes has never been fully understood despite the extensive structural information that has become available.^{4b,c,9} For example, consider the following: Brown suggested that the major diastereomer produced upon coordination of acetamidocinnamate to cationic Rh(I)P₂ is the more stable (and therefore less reactive), and this complex leads to a sterically more congested octahedral Rh(III) complex. This makes the catalytically relevant minor isomer more reactive, as observed experimentally. In sharp contrast, a more recent molecular mechanics calculation¹⁰ suggests that the diastereomeric octahedral Rh(III) complexes could not be reliably differentiated in energy from any other diastereomers and, in any case, cannot be viable on energy considerations alone. A highly distorted octahedral geometry is nonetheless possible, and tentative experimental support for this idea has emerged from a recent para-hydrogen induced polarization NMR (PHIP NMR) study of a related Rh-catalyzed hydrogenation.¹¹ A second explanation for the different reactivities is suggested by the different ¹⁰³Rh chemical shifts (and the attendant difference in electron density at Rh) in each of the two diastereomers.¹² How this might be related to the reactivities of the two diastereomers remains an open question.

(9) (a) McCulloch, B.; Halpern, J.; Thompson, M. R.; Landis, C. R. *Organometallics* **1990**, *9*, 1392. (b) Chan, A.; Pluth, J.; Halpern, J. *J. Am. Chem. Soc.* **1980**, *102*, 5952.

(10) Giovannetti, J. S.; Kelly, C. M.; Landis, C. R. *J. Am. Chem. Soc.* **1993**, *115*, 4040.

(11) Harthun, A.; Kadyrov, R.; Selke, R.; Bargon, J. *Angew. Chem., Int. Ed. Engl.* **1997**, *36*, 1103.

(12) Bender, B. R.; Koller, M.; Nanz, D.; von Philipsborn, W. *J. Am. Chem. Soc.* **1993**, *115*, 5889.

(13) (a) Brown, J. M.; Parker, D. *J. Org. Chem.* **1982**, *47*, 2722. (b) Brown, J. M.; Parker, D. *J. Chem. Soc., Chem. Commun.* **1980**, 342. (c) Kadyrov, R.; Freier, T.; Heller, D.; Michalik, M.; Selke, R. *J. Chem. Soc., Chem. Commun.* **1995**, 1745. (d) Heller, D.; Kadyrov, R.; Michalik, M.; Freier, T.; Schmidt, U.; Krause, H. W. *Tetrahedron Asymmetry* **1996**, *7*, 3025.

(14) In principle, the equilibration of intermediates in the Rh-catalyzed hydrogenation of acetamidocinnamate could also be studied by the type of experiments described in refs 4c and 12.

(15) (a) Inoguchi, K.; Morimoto, T.; Achiwa, K. *J. Organomet. Chem.* **1989**, *370*, C9–C12. (b) Jendralla, H. *Tetrahedron Lett.* **1991**, *32*, 3671. (c) Morimoto, T.; Chiba, M.; Achiwa, K. *Tetrahedron Lett.* **1989**, *30*, 735.

(16) Tanaka, M.; Ogata, I. *J. Chem. Soc., Chem. Commun.* **1975**, 735.

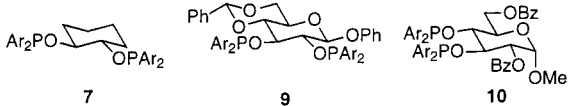
(17) (a) Selke, R.; Pracejus, H. *J. Mol. Catal.* **1986**, *37*, 213. (b) Unruh, J. D.; Christenson, J. R. *J. Mol. Catal.* **1982**, *14*, 19.

(18) Schrock, R. R.; Osborn, J. A. *J. Am. Chem. Soc.* **1971**, *93*, 2397.

Table 2. ^{31}P NMR Spectra of Phosphinite Ligands and Their Corresponding Rh(I) Complexes

entry	Ar in 7	ligand	^{31}P NMR (solvent)	complex	^{31}P NMR (solvent)
1	3,5-Me ₂ C ₆ H ₃	7a	111.5 (C ₆ D ₆)	Rh ⁺ [7a][COD]SbF ₆ ⁻	133.4 (d, 178) (CD ₂ Cl ₂)
2	Ph	7b	108.7 (C ₆ D ₆)	Rh ⁺ [7b][COD]SbF ₆ ⁻	131.0 (d, 177) (CDCl ₃) 129.7 (d, 178) (THF- <i>d</i> ₈) 133.3 (d, 179) (CD ₂ Cl ₂)
3	4-F-C ₆ H ₄	7c	105.3 (C ₆ D ₆)	Rh ⁺ [7c][COD]SbF ₆ ⁻	127.9 (d, 178) (C ₆ D ₆)
3	3,5-F ₂ C ₆ H ₃	7d	103.9 (C ₆ D ₆)	Rh ⁺ [7d][COD]SbF ₆ ⁻ Rh ⁺ [7d][COD]OTf ⁻	123.4 (d, 183) (CD ₂ Cl ₂) 120.7 (d, 183) (CD ₃ COCD ₃)
4	3,5-(CF ₃) ₂ C ₆ H ₃	7e	102.3 (C ₆ D ₆) 99.6 (THF- <i>d</i> ₈)	Rh ⁺ [7e][COD]SbF ₆ ⁻ Rh ⁺ [7e][COD]SbF ₆ ⁻ Rh ⁺ [7e][COD]OTf ⁻ [7e]Rh(<i>μ</i> -Cl)/2	131.5 (d, 219) (CD ₂ Cl ₂) 129.17 (d, 193) (THF- <i>d</i> ₈) 124.8 ^a (d, 178) (CD ₂ Cl ₂) (??) 127.25 (d, 182) (CD ₃ COCD ₃) 119.0 (d, 182) (CDCl ₃) 130.17 (d, 218) (CD ₂ Cl ₂) 127.67 (d, 218) (CD ₃ COCD ₃)
5	C ₆ F ₅	7f	85.0 (q, 41) CDCl ₃	Rh ⁺ [7f][COD]SbF ₆ ⁻	104.96 (d, 201) (CD ₂ Cl ₂)
6	C ₆ F ₅ /3,5-Me ₂ C ₆ H ₃	7g	86.72 (q, 39); 108.3 (CD ₂ Cl ₂)	Rh ⁺ [7g][COD]SbF ₆ ⁻	102.00 (ddm, 211, 28); 133.28 (dd, 168, 28) (CD ₂ Cl ₂)
7	C ₆ H ₅ /3,5-CF ₃ C ₆ H ₃	7h	99.5, 109.4 (C ₆ D ₆)	Rh ⁺ [7h][COD]SbF ₆ ⁻	125.5 (dd, 268, 36); 126.8 (dd, 243, 36) (CD ₃ COCD ₃)

^a Uncertain because the major product is [**7e**]Rh(*μ*-Cl)/2 in this solvent.

Table 3. Electronic Effects in Rh(I)-Catalyzed Hydrogenation of Dimethyl Itaconate^a


entry	Ar in ligands 7, 9, and 10	$\sum\sigma$ (σ_p or $2 \times \sigma_m$) ^b	7	9	10
1	3,5-Me ₂ C ₆ H ₃	-0.14	79.2 (<i>R</i>)	90.8 (<i>R</i>)	75.3 (<i>S</i>)
2	C ₆ H ₅	0.0	67.7 (<i>R</i>)	73.4 (<i>R</i>)	59.4 (<i>S</i>)
3	4-F-C ₆ H ₄	0.062	57.7 (<i>R</i>)	58.3 (<i>R</i>)	36.4 (<i>S</i>)
4	3,5-F ₂ -C ₆ H ₄	0.67	25.1 (<i>R</i>)	25.2 (<i>R</i>)	5.7 (<i>S</i>)
5	3,5-(CF ₃) ₂ C ₆ H ₃	0.86	0	5.5 (<i>R</i>)	

^a Reaction done in THF with 0.16 mol % catalyst at rt and 45 psi initial H₂ pressure. Isolated yield >99% in all cases. Ee measured by chiral GC on Chiraldex GTA column (see Experimental Section for details). ^b See ref 19.

perspective, the synthesis of the (*R*)-methylsuccinic acid using the ligand **9** in 90.8% ee represents one of the highest ee's obtained for this important class of compounds via hydrogenation using gaseous hydrogen. 4-Hydroxyproline-derived BPPM gives >97% (*S*) ee under transfer hydrogenation conditions.²⁰ However, the opposite enantiomer of this catalyst is not readily available for the production of the (*R*)-methylsuccinic acid derivatives. Ru(allyl)(acac-F₆)(BINAP) or Ru₂(BINAP)₂Cl₄(NEt₃) can be used for the synthesis of the (*R*)-isomer in ee's comparable to what is reported here (93 and 88% ee, respectively).²¹

Another key feature of the reaction is the dependence of the sense of asymmetric induction on the backbone chirality of the ligand. Thus, the bis-2,3-diarylphosphinite derived from a D-glucopyranoside (**9**) gives the (*R*)-enantiomer while the bis-3,4-diarylphosphinite (**10**) gives the (*S*)-enantiomer, albeit in lower selectivity, as com-

pared to the former. Thus, both enantiomers of the itaconates could, in principle, be obtained using ligands readily available from natural sources. The unnatural sugar L-glucose is more expensive than D-glucose, but nonetheless could also be used for the production of the (*S*)-isomer.

Hydrogenation of (*Z*)- α -N-Acetylcinnamic Acid Derivatives Using C₂-Symmetric Bis-phosphinites.

Hydrogenation of dehydroamino acid derivatives (eq 2) using cationic Rh(I) complexes of the C₂-symmetric ligands **7** were carried out in THF at 35–40 psi of hydrogen, and the results are tabulated in Table 4. All experiments were carried out with (1*S*,2*S*)-1,2-bis-arylphosphinoxyclohexane or its optical antipode, (1*R*,2*R*)-bis-phosphinite. Several important experimental observations warrant comments here. The most important conclusion is the remarkable electronic effect seen across the board for these C₂-symmetric ligands. Results for the prototypical dehydroamino acid ester, (*Z*)-methyl α -N-acetylcinnamate (entry 1), are illustrative. In comparison with the unsubstituted diphenylphosphinite **7b** (74.2% ee), the electron-deficient ligands 3,5-difluorophenyl (**7d**) and 3,5-bis-trifluoromethylphenyl (**7e**) phosphinite gave the lowest ee's in this series (49.6% ee and 25.9% ee, respectively). A more electron-rich 3,5-dimethylphenylphosphinite **7a** gave the highest ee (82.0% ee) of all the phosphinites under study. Most interestingly, pentafluorophenylphosphinite gave predominantly the opposite enantiomer of the amino acid ester.

Another interesting observation is related to the effect of an electronically unsymmetrical ligand. Two cases are reported in Table 4. Note that in entry 1 (Table 4) the bis-pentafluorophenylphosphinite (**7f**) gave 37.9% ee of the (*R*)-enantiomer and the bis-3,5-dimethylphenylphosphinite (**7a**) gave 82.0% ee of the (*S*)-enantiomer in this reduction. A mixed ligand **7g**, which carries one each of these diarylphosphinites, gave an ee of 79.3% (*S*), almost as good as the best observed selectivity.²² A similar result is obtained with a mixed ligand with phenyl and 3,5-bis-trifluoromethylphenylphosphinite (last column in Table

(19) Carroll, F. A. *Perspectives on Structure and Mechanism in Organic Chemistry*; Brookes/Cole: Pacific Grove, CA, 1998; p 384.

(20) Leitner, W.; Brown, J. M.; Brunner, H. *J. Am. Chem. Soc.* **1993**, *115*, 152.

(21) (a) Brown, J. M.; Brunner, H.; Leitner, W.; Rose, M. *Tetrahedron: Asymmetry* **1991**, *2*, 331. (b) Kawano, H.; Ikariya, T.; Ishii, Y.; Saburi, M.; Yoshikawa, S.; Uchida, Y.; Kumabayashi, H. *J. Chem. Soc., Perkin Trans. I* **1989**, 1571. (c) Burk et al. reported the use of the DuPhos series of ligands (>99% ee for dimethyl itaconate) while this publication was under review: Burk, M. J.; Bienewald, F.; Harris, M.; Zanotti-Gerosa, A. *Angew. Chem., Int. Ed. Engl.* **1998**, *37*, 1931.

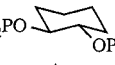
(22) The earliest known example of a related enhancement of enantioselectivity using electronically unsymmetrical ligand was recorded by Pracejus. Pracejus, H.; Pracejus, G.; Costisella, B. *J. Prakt. Chem.* **1987**, *329*, 235.

Table 4. Electronic Effects on Rh-Catalyzed Hydrogenation of α -N-Acetylcinnamic Acid Esters^a

Entry	Product	Aromatic group on phosphorus in ligand 7						
		Ar = Ar' = 3,5-di-Me-C ₆ H ₃ 7a	Ar = Ar' = Ph 7b	Ar = Ar' = 3,5-di-F-C ₆ H ₃ 7d	Ar = Ar' = 3,5-di-CF ₃ -C ₆ H ₃ 7e	Ar = Ar' = C ₆ F ₅ 7f ^b	Ar = 3,5-di-Me-C ₆ H ₃ , Ar' = C ₆ F ₅ 7g ^b	Ar = Ph, Ar' = 3,5-di-CF ₃ -C ₆ H ₃ 7h
1	N-Acetyl-4-phenyl alanine methyl ester	82.0 (S)	74.2 (S)	49.6 (S)	25.9 (S)	37.9 (R)	79.3 (S)	62.8 (S)
2	N-Acetyl-4-fluorophenyl alanine methyl ester	81.6 (S)	73.4 (S)	50.7 (S)	12.9 (S)	25.3 (R)	73.8 (S)	61.0 (S)
3	N-Acetyl-3,5-di-CF ₃ -phenyl alanine methyl ester	76.8 (S)	68.5 (S)	51.1 (S)	--	--	--	--

^a Quantitative yield, reactions done at rt and 35–40 psi H₂ pressure in THF. Ee's determined by GC (Chiracel-L-Val). See Experimental Section for details. ^b Studies done with (1*R*,2*R*)-bis-phosphinites. Sign inverted in table for comparison.

Table 5. Electronic Effects in Ni(0)-Catalyzed Hydrocyanation of MVN^a

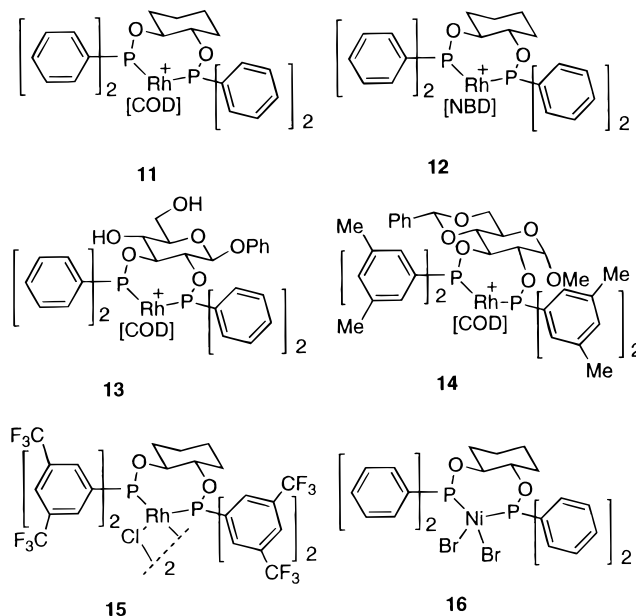
Entry	Ar ₂ PO-  -OPAr ₂ Ar	%ee ^b
1	3,5-Me ₂ -C ₆ H ₃	17 (S)
2	Ph	26 (S)
3	3-CF ₃ -C ₆ H ₄	33 (S)
4	3,5-F ₂ -C ₆ H ₃	38 (S)
5	3,5-(CF ₃) ₂ -C ₆ H ₃	35 (S)

^a For experimental procedure, see ref 5b. ^b Measured by chiral HPLC on a Chiracel OJ column.

4). We had previously seen related stereoelectronic effects on enantioselectivity in the Ni-catalyzed hydrocyanation of vinyl arenes. The highest enantioselectivity of asymmetric hydrocyanation was obtained for a ligand with an electronically unsymmetrical chelating bis-phosphinite.²³

The ee's were determined by gas chromatography, and they are highly reproducible. To verify the generality of these results, Rh-catalyzed hydrogenation of two other substrates, methyl esters of α -N-acetyl-4-fluorocinnamic acid (entry 2, Table 4) and of α -N-acetyl-3,5-bis(trifluoromethyl)cinnamic acid (entry 3, Table 4) were also carried out. As shown in Table 4, these substrates behave as expected, with the electron-withdrawing ligands giving the lowest enantioselectivity.

Ni(0)-Catalyzed Asymmetric Hydrocyanation of 2-Methoxy-6-vinylnaphthalene (MVN) Using *trans*-(1*S*,2*S*)-Diarylphosphinoxyclohexane. In 1994, we reported the most extensive studies of electronic effects on a carbon–carbon bond-forming reaction, viz. the Ni-catalyzed asymmetric hydrocyanation of vinyl arenes.^{5b} The 1,2-bis-diarylphosphinoxyclohexane system now allows the examination of these effects in a truly C₂-symmetric ligand. Asymmetric hydrocyanation of MVN was carried out in toluene at room temperature as described in our earlier paper,^{5b} and the enantioselectivities obtained are recorded in Table 5. As compared to the sugar-derived ligands (see Table 1, column 3) the ee's are lower; nonetheless, the amplification of selectivity by an electron-withdrawing group such as *m*-fluoro- or

**Figure 2.** Metal complexes of bis-1,2-diarylphosphinites.

m-trifluoromethyl is irrefutable from these data.²⁴ Thus, the electronic effect appears to be a more general phenomenon, not unique to the sugar-derived C₁-symmetric bisphosphinites.

Structures of the C₂-Symmetric Phosphinites and Their Rh(I) and Ni(II) Complexes. As pointed out earlier, the most convincing examples of amplification of enantioselectivity by electronic tuning of ligands employed C₁- or pseudo-C₂-symmetric ligands.^{23,26} While it was abundantly clear that the electronic effects of ligands played the most decisive role, a quantitative measure of this contribution, unaffected by backbone effects, was not possible because of the lack of C₂ symmetry (or another higher symmetry element). With the C₂-symmetric bis-(diaryl)phosphinites from cyclohexane-1,2-diol we can begin to address this question. In this connection, the structural aspects of the catalysts and intermediates are discussed at two levels: (i) First, solution- and solid-state structures of the precatalyst complexes **11–16** (Figure

(23) RajanBabu, T. V.; Casalnuovo, A. L. *J. Am. Chem. Soc.* **1996**, *118*, 6325.

(24) C₂-Symmetric bis-diarylphosphinites derived from (*S,S*)-tartraniol²⁵ are other examples where similar electronic effects on asymmetric hydrocyanation can be observed; see ref 23.

(25) Bourson, J.; Laureano, O. *J. Organomet. Chem.* **1982**, *229*, 77.

(26) (a) Asymmetric hydroformylation: RajanBabu, T. V.; Ayers, T. A. *Tetrahedron Lett.* **1994**, *35*, 4295. (b) Pd-catalyzed asymmetric allylation: Nomura, N.; Mermet-Bouvier, Y. C.; RajanBabu, T. V. *Synlett* **1996**, 745.

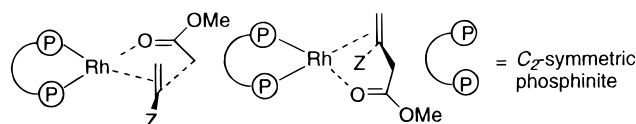


Figure 3. Diastereomers of [itaconate]Rh(I)P₂ complex.

2) will be discussed. The relevance of such ground-state structures to the catalytic process itself is, admittedly, of questionable value. Yet, conformations of ground-state precatalysts have been correlated with the sense of asymmetric induction²⁷ (vide infra), and as in any discussion of electronic effects on enantioselectivity, structural consequences of the electronic effects of ligands for the conformation of the catalyst should be considered. (ii) Next, our efforts to probe the effect of the *P*-aryl substituents on the diastereomeric equilibration of (*S,S*)-1,2-bis-diarylphosphenoxy-cyclohexane]Rh(+)[[dimethyl itaconate]SbF₆⁻ (Figure 3) and the attendant effect on enantioselectivity of dimethyl itaconate hydrogenation will be presented.

The itaconate reduction was chosen as an example of a prototypical Rh-catalyzed hydrogenation reaction because of its mechanistic similarity to the more important reduction of the dehydroamino acids and the ease of detection of the diastereomeric Rh(I) complexes (Figure 3) under the reaction conditions. Recall that in the case of the dehydroamino acid reductions these intermediates are more difficult to observe because the minor diastereomer has broad ³¹P peaks.^{13,28}

The ³¹P NMR spectra of the ligands and their Rh⁺(COD)LX⁻ complexes (L = bisphosphinite) clearly show the C₂-symmetric nature of these compounds (Table 2). For the ligands **7a–f** (Scheme 1), as expected only one ³¹P signal is observed. Upon coordination to Rh, the shifts move downfield. In addition, the coupling to ¹⁰³Rh is observed in each case. In two cases, in addition to the cationic complexes, we also prepared their neutral counterparts, {[**7d**][Rh(μ-Cl)]₂} and {[**7e**][Rh(μ-Cl)]₂} and recorded their ³¹P NMR. These complexes are also C₂-symmetric in solution as judged by the presence of a single ³¹P peak coupled only to ¹⁰³Rh. For a given complex, while there are considerable differences in the chemical shifts depending on which solvent is used, the multiplicities and the ¹J_{Rh–P} generally remain constant as the solvent is varied. The occurrence of P–P coupling (²J_{P–P}), which is seen in complexes of C₁-symmetric phosphinites such as **9**, but not of **7**, clearly indicates the C₂-symmetric

(27) (a) Kagan, H. B. Asymmetric synthesis using organometallic catalysts. In *Comprehensive Organometallic Chemistry*, Wilkinson, G., Stone, F. G. A., Abel, E. W., Eds.; Pergamon Press: Oxford, 1982; Vol. 8, p 463. (b) Knowles, W. S. *Acc. Chem. Res.* **1983**, *16*, 106. (c) Oliver, J. D.; Riley, D. P. *Organometallics* **1983**, *2*, 1032. (d) Bogdan, P. L.; Irwin, J. J.; Bosnich, B. *Organometallics* **1989**, *8*, 1450. (e) Brown, J. M.; Evans, P. L. *Tetrahedron* **1988**, *44*, 4905. (f) Pavlov, V. A.; Klabunovskii, E. I.; Struchkov, Y. T.; Voloboev, A. A.; Yanovsky, A. I. *J. Mol. Catal.* **1988**, *44*, 217. (g) Seebach, D.; Plattner, D. A.; Beck, A. K.; Wang, Y. M.; Hunziker, D.; Petter, W. *Helv. Chim. Acta* **1992**, *75*, 2171. (h) Sakuraba, S.; Morimoto, T.; Achiwa, K. *Tetrahedron: Asymmetry* **1991**, *2*, 597. For a highly pertinent, critical evaluation of these various models, see ref 10.

(28) (a) Chan, A. C. S.; Pluth, J. J.; Halpern, J. *J. Am. Chem. Soc.* **1980**, *102*, 5952. (b) Brown, J. M.; Chaloner, P. A. *J. Am. Chem. Soc.* **1980**, *102*, 3040. (c) Brown, J. M.; Chaloner, P. A. *Tetrahedron Lett.* **1978**, 1877. See, however, ref 4c.

(29) For other related systems, see: (a) Michalik, M.; Freier, T.; Schwarze, M.; Selke, R. *Magn. Reson. Chem.* **1995**, *33*, 835. (b) Brown, J. M.; Chaloner, P. A. *J. Am. Chem. Soc.* **1978**, *100*, 4307. (c) Berger, H.; Nesper, R.; Pregosin, P. S.; Rügger, H.; Würle, M. *Helv. Chim. Acta* **1993**, *76*, 1520.

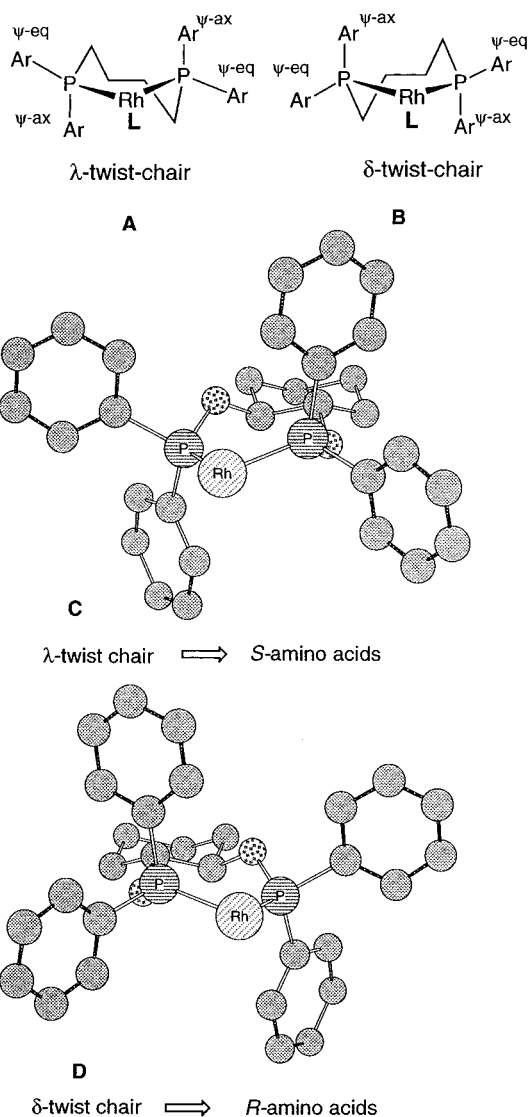


Figure 4. (A and B) Conformations of seven-membered cationic Rh chelates. (C and D) λ- and δ-conformations of C₂-symmetric vicinal [diaryl]phosphinite]Rh(I) complexes leading to *S* and *R* amino acids.

nature of the latter in solution. The ¹H NMR shows broad peaks for the allylic and olefinic hydrogens of the 1,5-cyclooctadiene (COD) ligand, suggesting slow rotation around the Rh–COD axis.²⁹

The ³¹P chemical shifts are dramatically different between complexes of the electron-rich and electron-poor ligands. For example, in CD₂Cl₂, complexes of the electron-rich ligands Rh⁺[**7a**][COD]SbF₆⁻ and Rh⁺[**7b**][COD]SbF₆⁻ have ³¹P shifts of δ 133.4 (d, *J* = 178 Hz) and 133.3 (d, *J* = 179 Hz). The complexes of electron-poor ligands, on the other hand, have the following chemical shifts: **7d**, δ 123.4 (d, *J* = 183 Hz); **7e**, δ 124.8 (d, *J* = 178 Hz); **7f**, δ 104.96 (d, *J* = 201 Hz). The chemical shifts and *J*_{Rh–P} coupling constants for Rh⁺[**7x**][CD₃OD]₂SbF₆⁻ are as follows: **7a**, δ 143.90 (*J* = 230 Hz); **7b**, δ 144.60 (*J* = 230 Hz); **7d**, δ 136.99 (*J* = 230 Hz); **7e**, δ 132.69 (*J* = 194 Hz). Phosphorus chemical shifts are dependent on both steric as well as electronic effects and the back-bonding properties of the metal.³⁰ At this stage, no

(30) (a) Tolman, C. A. *Chem. Rev.* **1977**, *77*, 313. (b) White, D.; Coville, N. J. *Adv. Organomet. Chem.* **1994**, *36*, 95.

discernible correlation between enantioselectivity or even reactivity can be drawn³¹ except to suggest that the precatalyst Rh(I) complexes that produce higher enantioselectivity have ³¹P chemical shifts in the more deshielded region in both the COD and bis-CD₃OD complexes. Significantly, in all cases the complex seems to maintain the C₂ symmetry in solution.

Crystal Structures of the Precatalysts with Electronically Different Diarylphosphinites. A number of studies aimed at clarifying the origin of enantioselectivity in Rh-catalyzed hydrogenation of acetamidoacrylic acid^{4,9,12} and itaconic acid derivatives^{11,13,20} have been carried out. Details of kinetics and thermodynamic aspects of key steps under a variety of reaction conditions are well-known. In the case of five- and seven-membered Rh-phosphine chelates, there exists a good empirical correlation between the λ- and δ-conformations of the starting Rh-catalyst and the sense of optical induction in the resulting amino acid, the λ-conformer of the precatalyst leading to the *S*-isomer and the δ-conformer to the *R*-isomer of the amino acid (Figure 4).²⁷ These conformations of the precatalyst, in the case of ideal C₂-symmetric ligands, present an asymmetric, alternating pseudoaxial and pseudoequatorial array of *P*-aryl groups around the metal, defining a chiral space. This leads to clockwise or anticlockwise skewing of the substrate providing kinetically and/or thermodynamically different diastereomeric intermediates, which ultimately results in enantioselective hydrogenation. The effect of such an asymmetric disposition of a coordinated ligand can be seen even in coordinated NBD or COD.^{27c,32,33} The forces that are responsible for the skewing of the dienes are thought to be important in the diastereoselective recognition and the subsequent enantioselective hydrogenation of prochiral olefins.³³ While the empirical relationship of the λ- vs δ-conformation of the precatalyst seems to hold good for five-membered chelates, it is more tenuous for seven-membered complexes. Because of the conformational mobility of seven-membered rings, the λ- and δ-conformations are sometimes poorly defined. Even for some five-membered Rh-chelates, several conformations are possible in the solid state, especially if different polymorphs are present. For example, Oliver and Riley^{27c} have described one case where the Rh⁺-complex of (*R*)-1,2-bis(diphenylphosphino)-1-cyclohexylethane ((*R*)-cycphos) exists in two different polymorphic forms and one of the polymorphs has two conformations for the complex (Figure 5). Nonetheless, all three arrangements of the precatalyst can be approximately defined as belonging to the λ-conformation shown in Figure 4 (ω and ω', as defined in Figure 7, are -6.7/-7.7, -22/-3, and -14.2/-11.2, respectively, for these cationic structures). Accordingly, very high enantioselectivity for the formation of the (*S*)-isomer is observed in the asymmetric hydrogenation of acetamidoacrylic acid derivatives. As these authors have correctly pointed out, these results clearly show that the coordinated ligands need not form a rigid complex. There is often considerable flexibility in the conformations of the ligand backbone, and this could have important implications for enantioselectivity.

(31) In an NMR study of the diastereomeric Rh-complexes of acetamidoacrylates Philipsborn also came to the same conclusions. See ref 12 and the corresponding Supplementary Material.

(32) Armstrong, S. K.; Brown, J. M.; Burk, M. J. *Tetrahedron Lett.* **1993**, *34*, 879.

(33) Kyba, E. P.; Davis, R. E.; Juri, P. N.; Shirley, K. R. *Inorg. Chem.* **1981**, *20*, 3616.

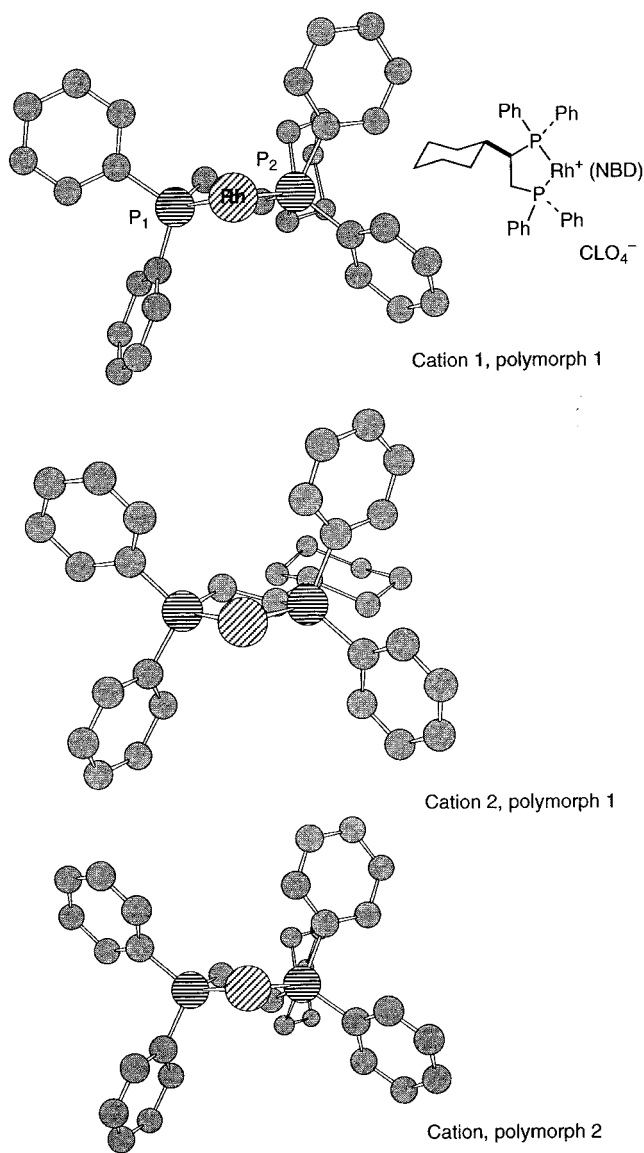


Figure 5. Cations of Rh⁺[(*R*)-cycphos][NBD]ClO₄⁻ from different polymorphs.^{27c} All structures are roughly of the λ-conformation shown in Figure 4. NBD and the anions are omitted for clarity.

In light of the above discussion, it is imperative that any discussion of electronic effects of phosphorus ligands should first address the effect of electronic changes on the ground-state conformations of the catalyst. For example, could one trace the difference in the behavior of electron-rich and electron-poor phosphinites to a difference in the ground-state conformations of the respective Rh chelates? To explore this possibility, we conducted a crystallographic analysis of a number of Rh-phosphinite complexes. After repeated attempts we were able to grow good-quality crystals of compounds **11**, **12**, **15**, and **16** (Figure 2). The structures of these complexes were solved by standard techniques.³⁴ While our study was in progress, Selke et al. reported³⁵ the structure of

(34) See the Supporting Information for details. The authors have deposited atomic coordinates for the structures of **11**, **12**, **15**, and **16** with the Cambridge Crystallographic Data Centre. The coordinates can be obtained, upon request, from the Director, CCDC, 12 Union Road, Cambridge CB 1EZ, U.K.

(35) Kempe, R.; Schwarze, M.; Selke, R. *Zeitschrift. Kristal.* **1995**, *210*, 555.

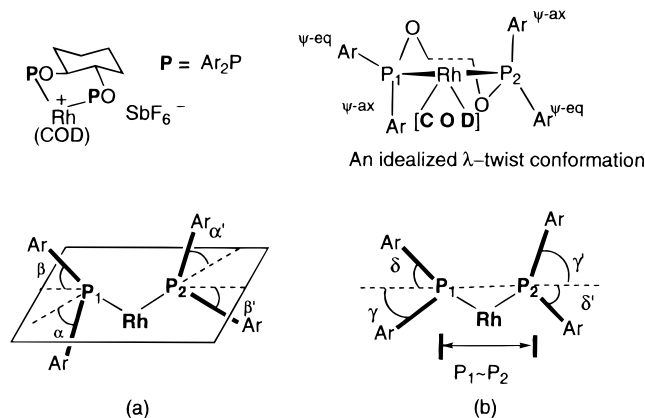


Figure 6. Definitions of angles and distances used in Table 6. (a) α and β represent lower of the two angles between the plane defined by P_1 , Rh, and P_2 and the P-Ar bond. The front (f)/rear (r) designations refer to the positioning of the P-aryl groups with respect to a plane perpendicular to the $\text{P}_1\text{-Rh-P}_2$ plane that passes through P_1 and P_2 . (b) Angles δ and γ are formed between the P-Ar bond and the line connecting P_1 and P_2 .

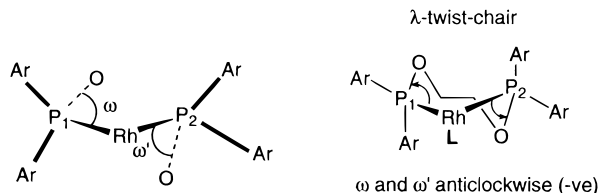


Figure 7. Definition of ω and ω' . The dihedral angle between O-P_1 and Rh-P_2 is ω , and the corresponding angle between O-P_2 and Rh-P_1 is ω' . When viewed from the front, if the smallest angle rotation from $\text{P}_2\text{-Rh}$ to $\text{P}_1\text{-O}$ is clockwise ω is positive and if it is anticlockwise ω is negative. For the λ conformation both ω and ω' will be negative and for the δ -conformation both will be positive.

a related complex, **13**. The structure of **14** was not fully solved because of major crystal disorders; nonetheless, the parameters we were able to extract enabled us to compare conformational features of this complex with others in the series.

Chem3D versions (created from a PDB format) of the crystal structures of **11–16** are shown in Figures 8–13. Selected interatomic distances and intramolecular angles are shown in Tables 6 and 7. In reporting these data, we have used the conventions used by Pavlov^{27f} and Seebach^{27g} (Figures 6 and 7).

Complexes **11–14** form discrete Rh^+ chelates in the solid state, with no interaction showing between the counteranion and Rh. As expected, all are nearly square planar with $\text{P}_1\text{-Rh-P}_2$ near 90° in all cases.

As shown in Figure 8, the conformation of the cationic Rh^+ -complex of *trans*-(1*S*,2*S*)-1,2-di-*O*-diphenylphosphinocyclohexane depends on the ancillary ligand present. With 1,5-cyclooctadiene as the ancillary ligand the complex exists in an idealized λ -twist-chair conformation with the endocyclic ω and ω' angles -19° , -36° and -22° , -30° , respectively. Note that the complex **11** shows only a single ^{31}P peak in the NMR, indicating its near- C_2 -symmetric nature. In the solid-state structure of **11** the COD ligand shows a clockwise skew rotation with respect to the $\text{P}_1\text{-Rh-P}_2$ plane.^{32,33} The Rh-complex **11**, in

conformity with the generalizations,²⁷ gives (*S*) amino acids in typical hydrogenation experiments (Table 4, under **7a** and **7b**).

Substituting the auxiliary 1,4-cyclooctadiene ligand in the complex **11** by norbornadiene brings about substantial changes in the solid-state structure of the resulting complex (Figure 8). The crystal has two distinct conformations for the cationic Rh complex. Cation 1, **12(Rh₁)**, has a λ -twist-chair conformation, roughly comparable to the COD complex **11**, while cation 2, **12(Rh₂)**, has a twist-boat conformation difficult to define by the λ/δ convention.

The λ -twist-chair conformation for a metal complex of the *trans*-(1*S*,2*S*)-1,2-di-*O*-diphenylphosphinocyclohexane appears to be general. For example, an almost perfectly C_2 -symmetric complex **16** is formed upon reaction of the ligand with $\text{NiBr}_2\cdot\text{DME}$ complex. As judged from the structural parameters α , β , γ , and ω (Tables 6 and 7, entries 1 and 8), the Rh(I)-complex **11** and the Ni(II)-complex **16** (Figure 9) have identical conformations for the seven-membered ring.

The twist-boat conformation **12(Rh₂)** of the L_2Rh^+ - (NBD) complex also appears in catalytically relevant complexes **13** and **14** (Figure 10). A careful inspection of the geometric parameters associated with structures of **13** and **14** (Tables 6 and 7) reveal that the values of α , β , δ , and γ and the positioning of the P-aryl groups in both of these complexes are comparable. Both of these complexes derived from C_1 -symmetric ligands prepared from D-glucose and are known to give very high enantioselectivities for the production of *S*-phenylalanine methyl ester from the corresponding dehydroamino acids. It is interesting to note that the alignment of the sugar backbone is clearly different in each case. To maintain a nearly identical seven-membered chelate conformation for **13** and **14**, C_1 of the sugar is kept to the right of the viewer in the former, whereas C_4 is to the right of the viewer in **14**. Since both of these complexes give excellent enantioselectivity³⁶ (95% and 90% ee's respectively), one may reasonably conclude that the chirality of the carbons on the sugar frame to which the phosphinoxy groups are attached, rather than the rest of the sugar backbone, is the more important control element, an idea that we have since used in the synthesis of both (*S*)- and (*R*)-amino acids from D-glucose.⁶ Yet another aspect of the structure of the 3,5-dimethylphosphinite is the possible hindered rotation around the two P-aryl groups on the β -face (Ar_1 and Ar_2 in **14**). An examination of the model suggests that the *m*-methyl groups from these two aryl groups could approach within van der Waals radii in certain rotamers. No two other aryl groups have this problem. Pregosin recently compiled a number of asymmetric reactions where the 3,5-dimethylphenyl motif in the metal catalysts have been shown to have a beneficial effect for high enantioselectivity.³⁷ It would be interesting to explore what role, if any, restricted rotation plays in these instances.

Finally, the solid-state structure of a precatalyst from 1,2-bis-3,5-bis-trifluoromethylphenylphosphinite (**15**) is shown in Figure 11. We were unable to grow good quality crystals of the corresponding COD or NBD complexes. Conditions under which the COD and NBD complexes **11**, **12**, and **14** were formed (addition of stoichiometric amount of a CH_2Cl_2 solution of the ligand to $(\text{COD})_2\text{Rh}^+$

(36) Selke, R. *J. Organomet. Chem.* **1989**, 370, 249.

(37) Trabesinger, G.; Albinati, A.; Feiken, N.; Kunz, R. W.; Pregosin, P. S.; Tschoerner, M. *J. Am. Chem. Soc.* **1997**, 119, 6315.

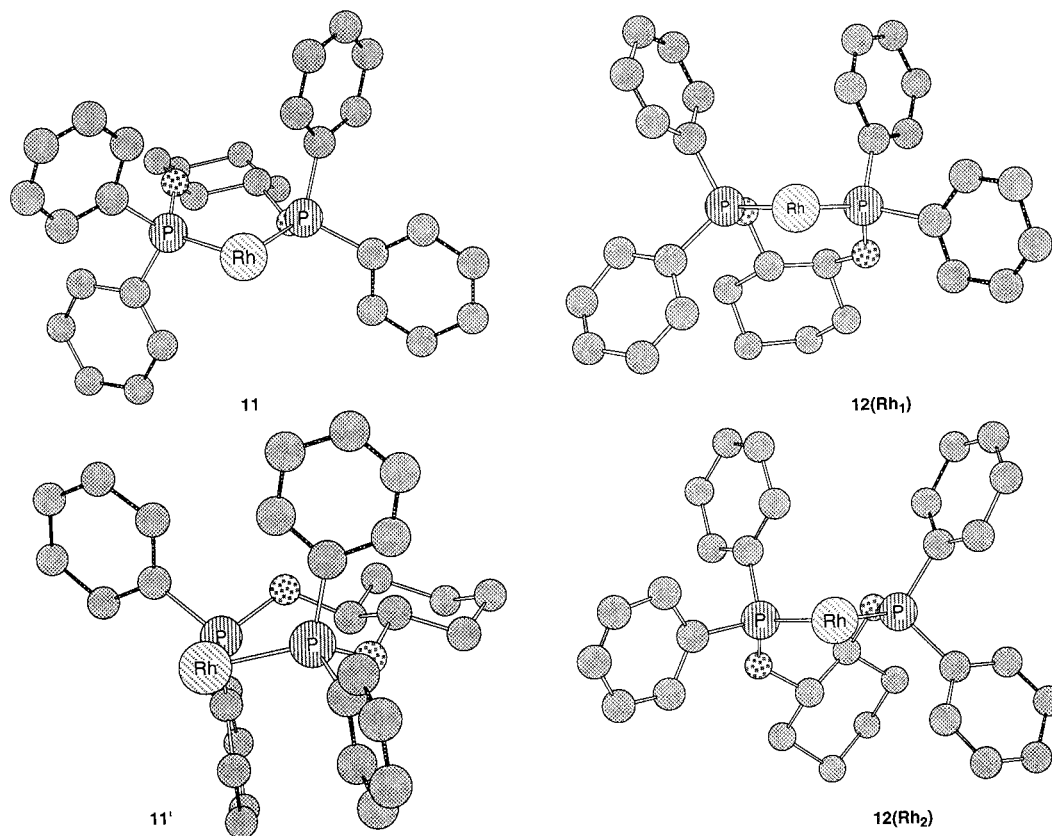


Figure 8. Crystal structures of **11** and **12** (Figure 2). **11** and **11'** are two perspectives. **12(Rh₁)** and **12(Rh₂)** are two distinct conformations in the crystal.

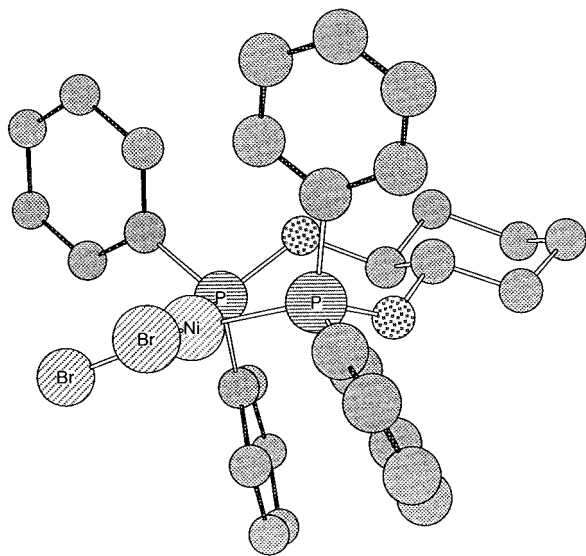


Figure 9. Crystal structure of **16** (Figure 2).

or (NBD)₂Rh⁺) produced only the chloride-bridged dimer **15**. Highly electron-deficient Rh abstracts a chlorine from the solvent to produce the bridged dimer. We were able to prepare the cationic complex in nonchlorinated solvents (see Table 2), but this complex could not be crystallized. The structure of **15** consists of two almost identical RhP₂ fragments as shown in Figure 11. A close examination of the seven-membered chelate (**15B**) shows that the ring has approximately the same twist-boat conformation of **12(Rh₂)**, **13**, and **14**. Comparison of the structural parameters α , β , α' , β' , γ , δ , γ' , δ' , ω , and ω'

with those of **13** and **14** is especially revealing. For **13**, **14**, and **15** these values (Table 6, entries 4, 5, 6, and 7; Table 7, entries 4, 5, 6, and 7) are as follows:

13: 2 (f), 56 (r), 88 (–), 26 (–), 11, 63, 51, 17, 63, –27

14: 8 (f), 70 (r), 71 (–), 52 (–), 11, 57, 40, 29, 53, –3

15: 2 (f), 63 (r), 87 (–), 30 (–), 12, 58, 44, 21, 59, –24

Recall that **13** and **14**, which incorporate relatively electron-rich *P*-aryl groups, are excellent precatalysts for hydrogenation of dehydroamino acids. In sharp contrast, Rh complex **15** with its electron-deficient CF₃ groups is a very poor precatalyst. Yet they are structurally similar in the ground state. Therefore, to a first approximation, it is reasonable to conclude that the electronic enhancement of enantioselectivity is *not due to changes in the ground-state conformations*.

Do Electronic Effects of Ligands Alter the Ratio of Major to Minor Diastereomers? Halpern's classic studies^{4a} on hydrogenation have shown that two factors that are most important in asymmetric induction in Rh-catalyzed hydrogenation are the ratio of the initially formed diastereomers (Figure 1) and the reactivity (oxidative addition of hydrogen, which converts these Rh(I) complexes into octahedral Rh(III) intermediates) of these intermediates. As we have reasonably concluded in the previous section, if the electronic effects do not alter the ground-state conformations of the precatalysts, the next logical question is how electronic variations in a ligand affect these two factors. Here we describe our attempts to provide partial answers to these questions. We decided to examine the ratio of the two diastereomers as a function of electronic effects of the ligand in the

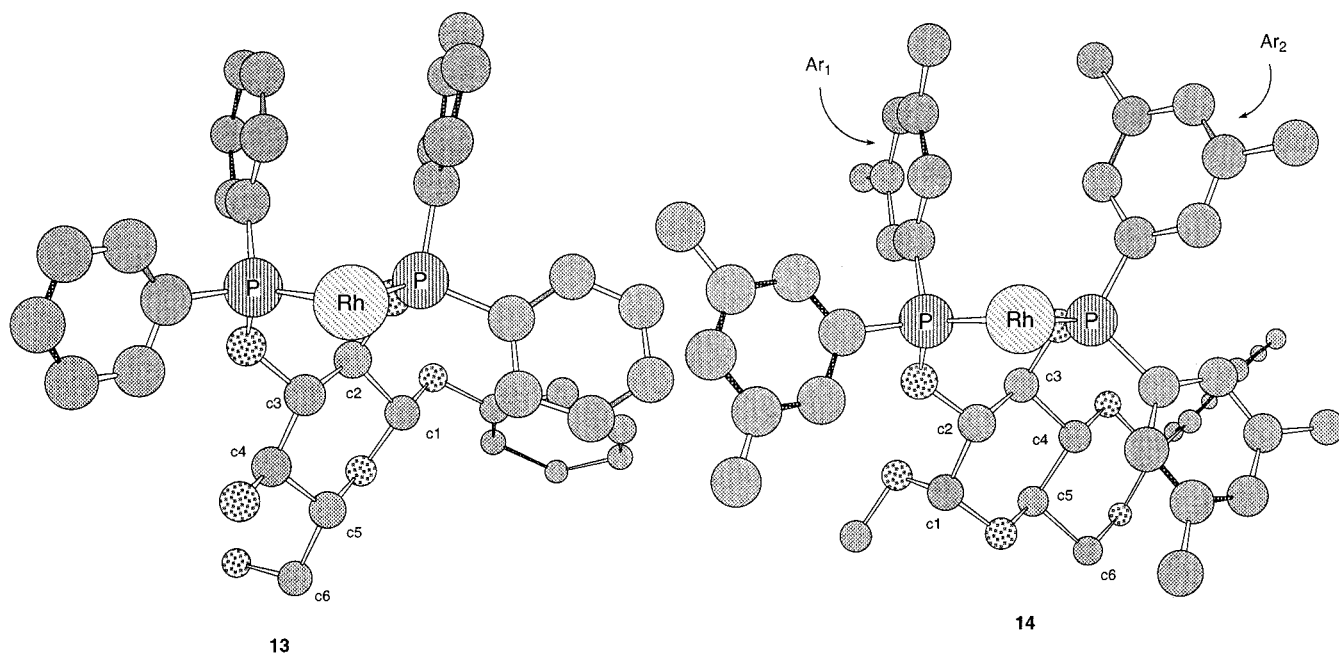


Figure 10. Crystal structures of complexes **13** (from Selke et al.³⁵) and **14**. COD, counterion, and the H's are omitted for clarity.

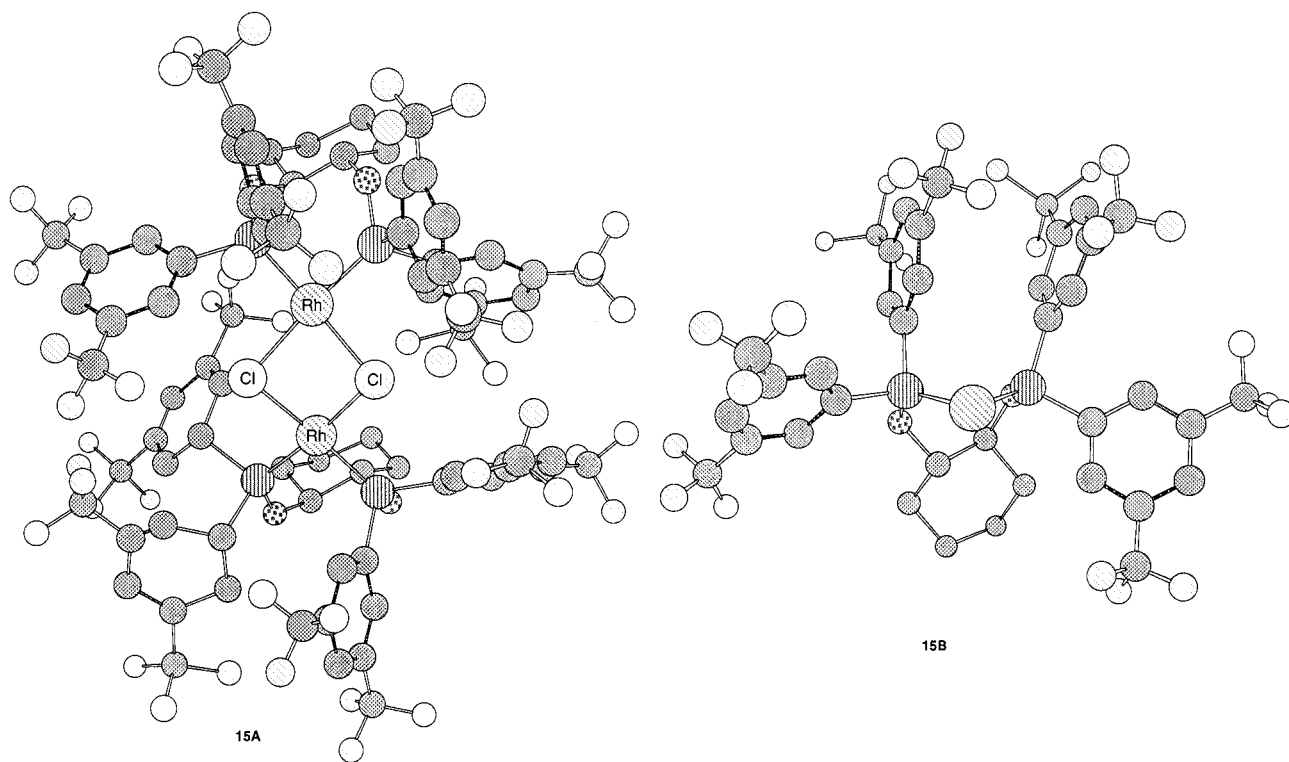


Figure 11. Crystal structure of **15** (Figure 2). The conformation of both halves of the dimer are approximately the same. **B** shows the details of the seven-membered chelate.

hydrogenation of dimethyl itaconate (eq 3). The itaconate system, rather than the α -acetamidocinnamate, was chosen for this study since the two reactions are mechanistically similar, yet the Rh(I)-substrate complexes in the former are easier to observe by ^{31}P NMR spectroscopy.¹³

We prepared the [dimethyl itaconate]Rh⁺[phosphinite] complexes with ligands **7a**, **7b**, **7d**, and **7e** (Scheme 1) by removal of the COD ligand by hydrogenation of the appropriate precatalyst from [COD]Rh⁺[phosphinite] in CD₃OD followed by addition of an excess of dimethyl

itaconate (Scheme 2). The ^{31}P NMR spectra were recorded at various temperatures between 303 and 208 K. These are shown in Figures 12–15.

The unsubstituted bis-diphenylphosphinite **7b** at 303 K shows a clean doublet (δ 144.6, $J_{\text{Rh-P}} = 230$ Hz) characteristic of [CD₃OD]₂Rh⁺[**7b**] except for a very broad small peak at δ 125.5–128.5.^{13c} Judging from the chemical shift of this minor peak and changes it undergoes upon cooling (vide infra), it is conceivable that this signal is due to *all* the phosphorus atoms from the diastereomeric complexes (Figure 3) that are under rapid equilibrium.

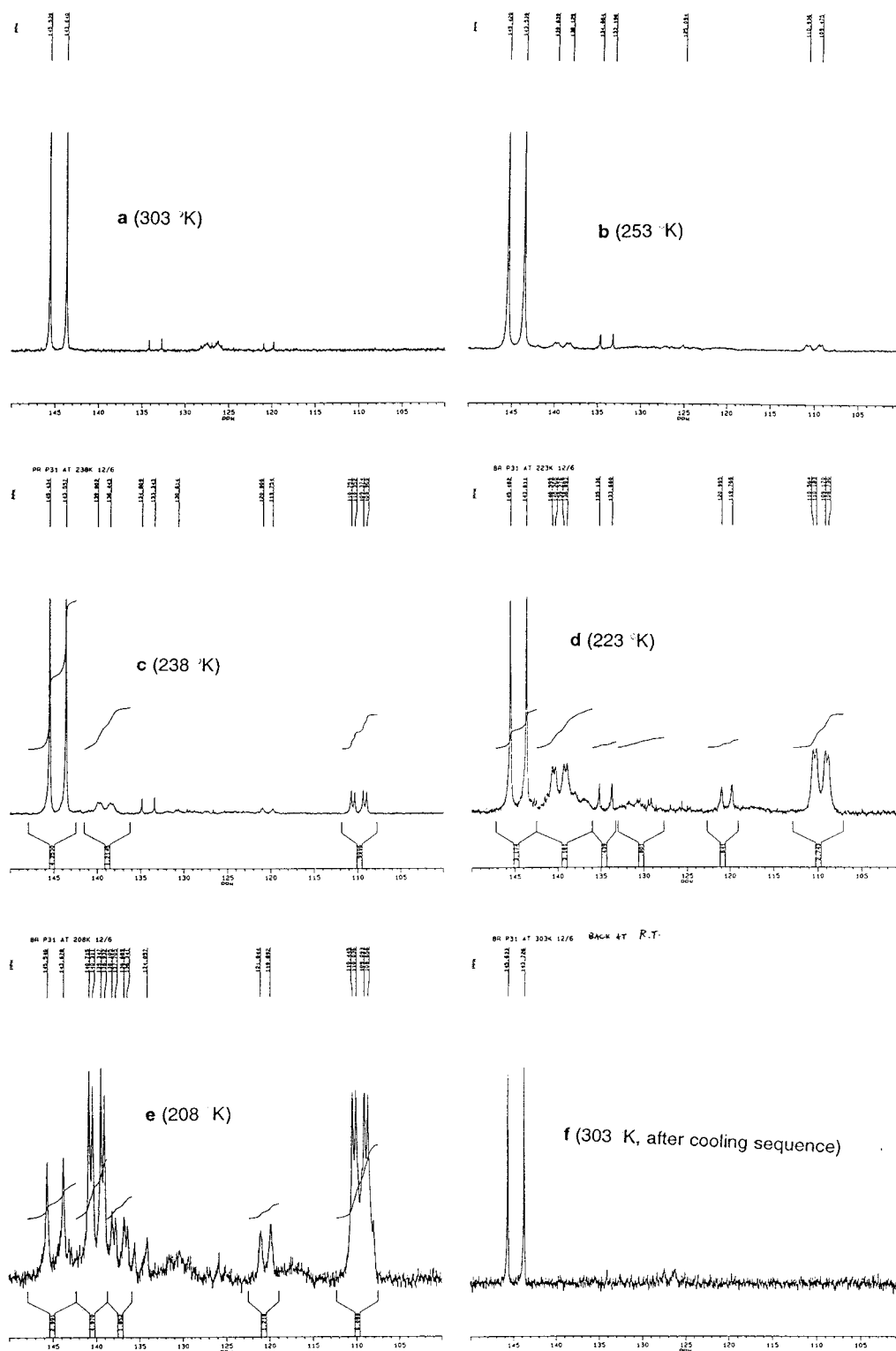


Figure 12. Temperature-dependent ^{31}P NMR spectra of diastereomers of [dimethyl itaconate] Rh^+ [**7b**].

Upon cooling, in accordance with the observations of Brown^{13b} and Selke,^{13c} signals due to the two distinct phosphorus atoms of the diastereomers of [dimethyl itaconate] Rh^+ [**7b**] begin to appear (Figure 12b–e). At 253 K (Figure 12b), two broad doublets of multiplets (of equal intensity) are seen at δ 108.5–111.5 ($J_{\text{Rh-P}} = 170$ Hz) and 137.5–140.5 ($J_{\text{Rh-P}} = 208$ Hz). The broadness of these peaks and the absence of discernible P–P coupling at this temperature is probably due to the fast intermolecular exchange

between the major and minor diastereomers (Figure 3).^{13c} Upon cooling to 238 K (Figure 12c), the high-field signals become sharp (δ 109.9, $J_{\text{Rh-P}} = 169$ Hz, $J_{\text{PP}} = 49$ Hz) while the low-field signals still remain as a doublet of multiplets (δ 137.0–141.0, $J_{\text{Rh-P}} = 177$). The ratio of intensities of the signals due to $[\text{CD}_3\text{OD}]_2\text{Rh}^+$ [**7b**] and those of the itaconate adducts at this temperature is approximately 2:1. At 223 K (Figure 12d), the proportion of the itaconate adducts increases at the expense of the

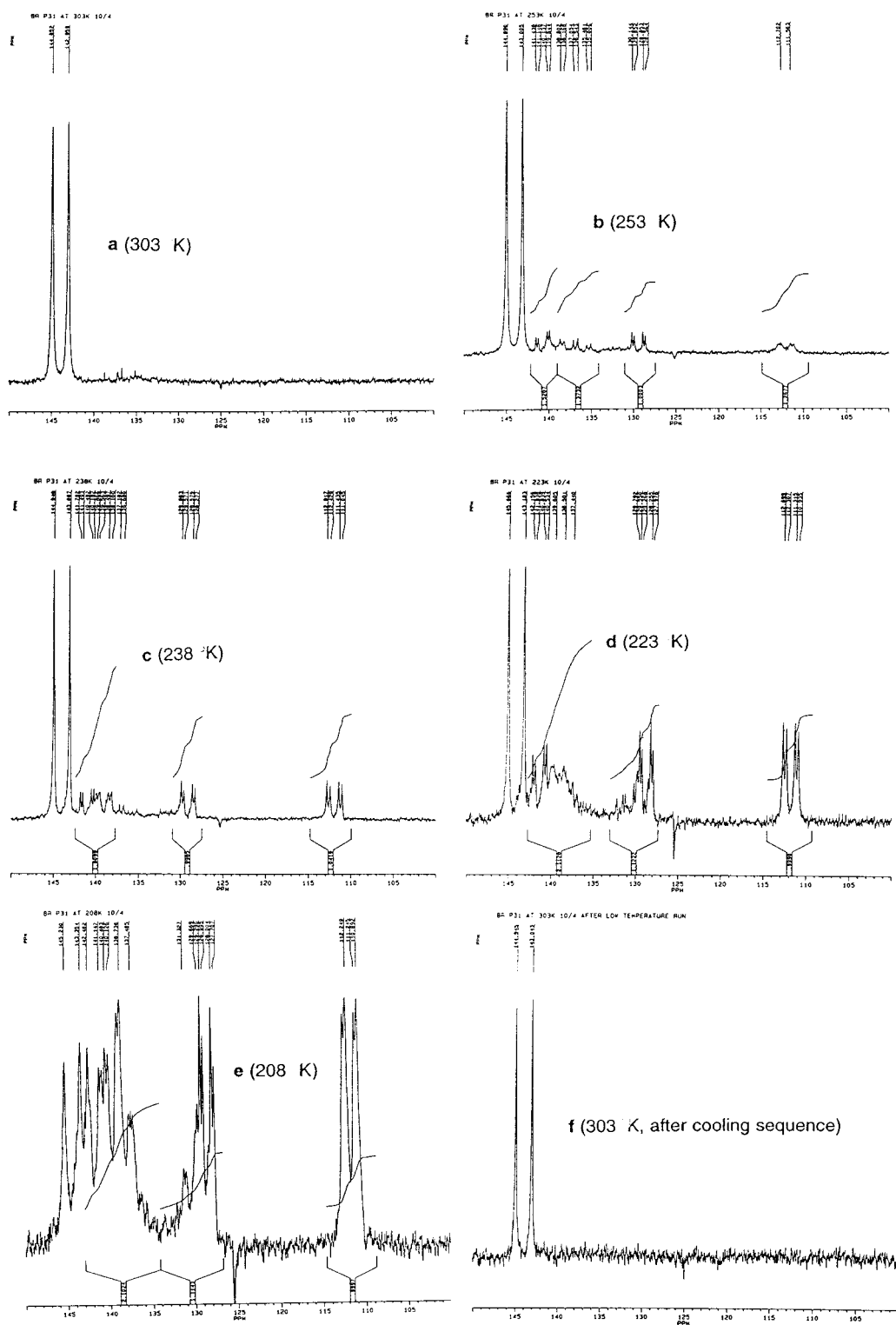


Figure 13. Temperature-dependent ^{31}P NMR spectra of diastereomers of [dimethyl itaconate] Rh^+ [7a].

solvate complex (the ratio of the solvate/itaconate adducts 1:2), and the low-field phosphorus signals begin to further broaden and resolve (δ 136.0–142.0, with a doublet of multiplets centered around δ 140 ($J_{\text{Rh-P}} = 164$ Hz)). The high-field signal around δ 110, possibly the phosphorus trans to the olefin,^{4c} broadens, indicating that indeed this could arise from a major and a minor peak. At 208 K (Figure 12e), only 20% of the ^{31}P intensity is due to the $[\text{CD}_3\text{OD}]_2\text{Rh}^+$ [7b]. As observed by Selke et al.,^{13c} the high-field phosphorus signal shows no change except for

further line broadening. At this temperature, the signals between δ 137 and 142 are fairly well resolved into two doublets of doublets, presumably arising from the major and minor diastereomers of the [itaconate] Rh^+ [7b] complex,^{13c} and we can now estimate the ratio of the major to minor diastereomer as 2.6:1. Finally, upon warming the solution to 303 K, the original ratio of the Rh-complexes is restored (Figure 12f).

The [itaconate] Rh^+ [7a] complex was prepared in the same fashion, and the temperature-dependent ^{31}P NMR

Table 6. Selected Interatomic Distances (Å) and Angles (deg) for Phosphinite Complexes^a

entry	complex	α	β	α'	β'	γ	δ	γ'	δ'	P–P	P ₁ –Rh–P ₂	Rh–P ₁	Rh–P ₂
1	11	75 (r)	47 (f)	90 (r)	31 (f)	41	29	48	21	3.179	90.2	2.239	2.250
2	12 (Rh ₁)	52 (–)	74 (–)	72 (r)	11 (f)	29	41	54	17	3.243	91.8	2.247	2.270
3	12 (Rh ₂)	8.3 (f)	72 (r)	64 (–)	54 (–)	15	58	37	31	3.184	90.2	2.238	2.258
4	13 ^b	2 (f)	56 (r)	88 (–)	26 (–)	11	63	51	17	3.150	88.2	2.250	2.276
5	14	8 (f)	70 (r)	71 (–)	52 (–)	11	57	40	29	3.171	89.8	2.207	2.283
6	15 (Rh ₁)	2 (f)	63 (r)	87 (–)	30 (–)	12	58	44	21	3.017	88.6	2.161	2.157
7	15 (Rh ₂)	1 (f)	62 (r)	88 (–)	26 (–)	11	60	47	20	3.025	88.8	2.156	2.165
8	16 ^c	79 (r)	45 (f)	85 (r)	37 (f)	44	27	46	22	3.165	95.2	2.133	2.153

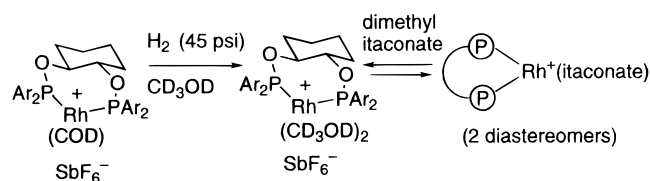
^a See Figures 6 and 7 for description of angles and distances: (f) front, (r) rear, (–) position uncertain. ^b From Selke.³⁵ ^c NiBr₂ complex.

Table 7. Dihedral Angles^a ω and ω' in Rh Phosphinite Complexes

entry	complex	ω	ω'
1	11	–19	–36
2	12 (Rh ₁)	55	1
3	12 (Rh ₂)	7	–57
4	13 ^b	63	–27
5	14	53	–3
6	15 (Rh ₁)	59	–24
7	15 (Rh ₂)	56	–29
8	16 ^c	–22	–30

^a See Figure 7 for definitions (after Pavlov et al.^{27f}). ^b From Selke.³⁵ ^c NiBr₂ complex.

Scheme 2. Synthesis of [Phosphinite]Rh(I)-Itaconate Complexes



spectra obtained are shown in Figure 13. At 303 K, only signals due to $[\text{CD}_3\text{OD}]_2\text{Rh}^+[\mathbf{7a}]$ that appear as a doublet at δ 143.9 ($J_{\text{Rh-P}} = 230$ Hz) are visible. Cooling the methanolic solution to 253 K results in the formation of three sets of new peaks. The highest field signal is a broad doublet of multiplets reminiscent of the high-field signal from the complex $[\text{itaconate}]\text{Rh}^+[\mathbf{7b}]$. At 238 K, the spectrum is well resolved (Figure 13c), and the major and minor diastereomers can be easily identified. The major diastereomer has a doublet of doublets at δ 111.9 ($J_{\text{Rh-P}} = 168$ Hz, $J_{\text{PP}} = 47$ Hz) and another poorly resolved doublet of doublets at δ 139.0 ($J_{\text{Rh-P}} = 166$ Hz), whereas the minor diastereomer has two doublet of doublets at δ 129.1 ($J_{\text{Rh-P}} = 157$ Hz, $J_{\text{PP}} = 35$ Hz) and 140.9 ($J_{\text{Rh-P}} = 157$ Hz, $J_{\text{PP}} = 35$ Hz). For this ligand, the ratio of the major to minor diastereomer at this temperature as determined from the respective ³¹P signals is approximately 1:1. Further cooling results in the appearance of even more peaks (Figure 13c–e), and one can only speculate the origin of these peaks. As pointed out earlier, the 3,5-dimethylphenylphosphinite has the possibility of some restricted rotation around the P-aryl bond, and these rotomers could be responsible for the new peaks. At 208 K, where one can reliably estimate the major/minor ratio of diastereomers for the $[\text{itaconate}]\text{Rh}^+[\mathbf{7b}]$ complex (= 2.6:1), the corresponding ratio for the $[\text{itaconate}]\text{Rh}^+[\mathbf{7a}]$ complex is at least 1:1 (Figure 13e). In any case, there is a clear difference in the relative proportion of the major and minor diastereomers of the P₂Rh-itaconate complex, as a function of the P-aryl substituent of the ligand. For the 3,5-dimethylphenylphosphinite, **7a**, which gave the highest ee, there is more

of the catalytically relevant minor diastereomer at equilibrium. This could at least in part explain the pronounced enantioselectivity with this ligand.

Further verification of this hypothesis was sought with a temperature-dependent ³¹P NMR study of the diastereomers of $[\text{dimethylitaconate}]_2\text{Rh}^+[\mathbf{7d}]$ and $[\text{dimethylitaconate}]_2\text{Rh}^+[\mathbf{7e}]$, each with an electron-deficient ligand. The results for the 3,5-difluorophenylphosphinite are shown in Figure 14. The ³¹P signal for $[\text{CD}_3\text{OD}]_2\text{Rh}^+[\mathbf{7d}]$ appears at δ 137.0 ($J_{\text{Rh-P}} = 230$ Hz). In sharp contrast to the more electron-rich phosphinite, **7a**, the electron-deficient **7d** appears to induce coordination of the itaconate to Rh even at 303 K. A very broad peak at δ 111–114 was assigned to fast equilibrating mixtures of the itaconate complexes based on the effect of temperature on this signal. Upon cooling first to 253 K, and subsequently to 238 and 223 K (Figure 14b–d), this broad peak is replaced by four sets of peaks at δ 96–101, 105–108, 112–115, and 120–127. Unfortunately, assignment of these peaks to the major and minor diastereomers has not been possible because of the complicated coupling patterns (some of them undoubtedly due to the long-range P–F couplings). Another complication is the appearance of peaks at δ 134–138 under the signals due to the solvate complex. Even though the changes in the spectrum are intractable, the reversible changes are highly reproducible, as shown by the last spectrum (Figure 14f), obtained upon warming the solution to 303 K. No reliable quantitative comparison to the 3,5-dimethylphosphinite system ($[\text{dimethylitaconate}]_2\text{Rh}^+[\mathbf{7a}]$) is possible.

Finally, the itaconate complexes with the most electron-deficient ligands, viz., the 1,2-(bis-bis-(3,5-bis-trifluoromethylphenyl)phosphinoxy)cyclohexane (**7e**) were studied. Recall that this ligand gave essentially 0% ee in the hydrogenation. The most striking feature of the spectrum at 303 K (Figure 15a) is the large proportion of the dimethyl itaconate complex present in solution vis-à-vis the spectra when the ligands **7a** and **7b** (or even **7d**) are employed. The solvate complex $[\text{CD}_3\text{OD}]_2\text{Rh}^+[\mathbf{7e}]$ appears at δ 132.7 ($J_{\text{Rh-P}} = 194$ Hz), and the broad doublet of multiplets due to the fast-exchanging mixture of itaconate complexes appears at δ 122–126 (Figure 15a). Further cooling of this mixture to 253 K, and subsequently to 238 K, results in what appears to be a symmetrical movement of the ³¹P signals to either side of the broad peak seen at room temperature. Even at 208 K, the spectrum is poorly resolved, and the intermediate complexes appear to be in fast equilibrium. In sharp contrast to the electron-rich systems, no discernible P–P or even Rh–P couplings can be extracted from these spectra. Another significant difference between the electron-rich and electron-poor systems is the relatively large

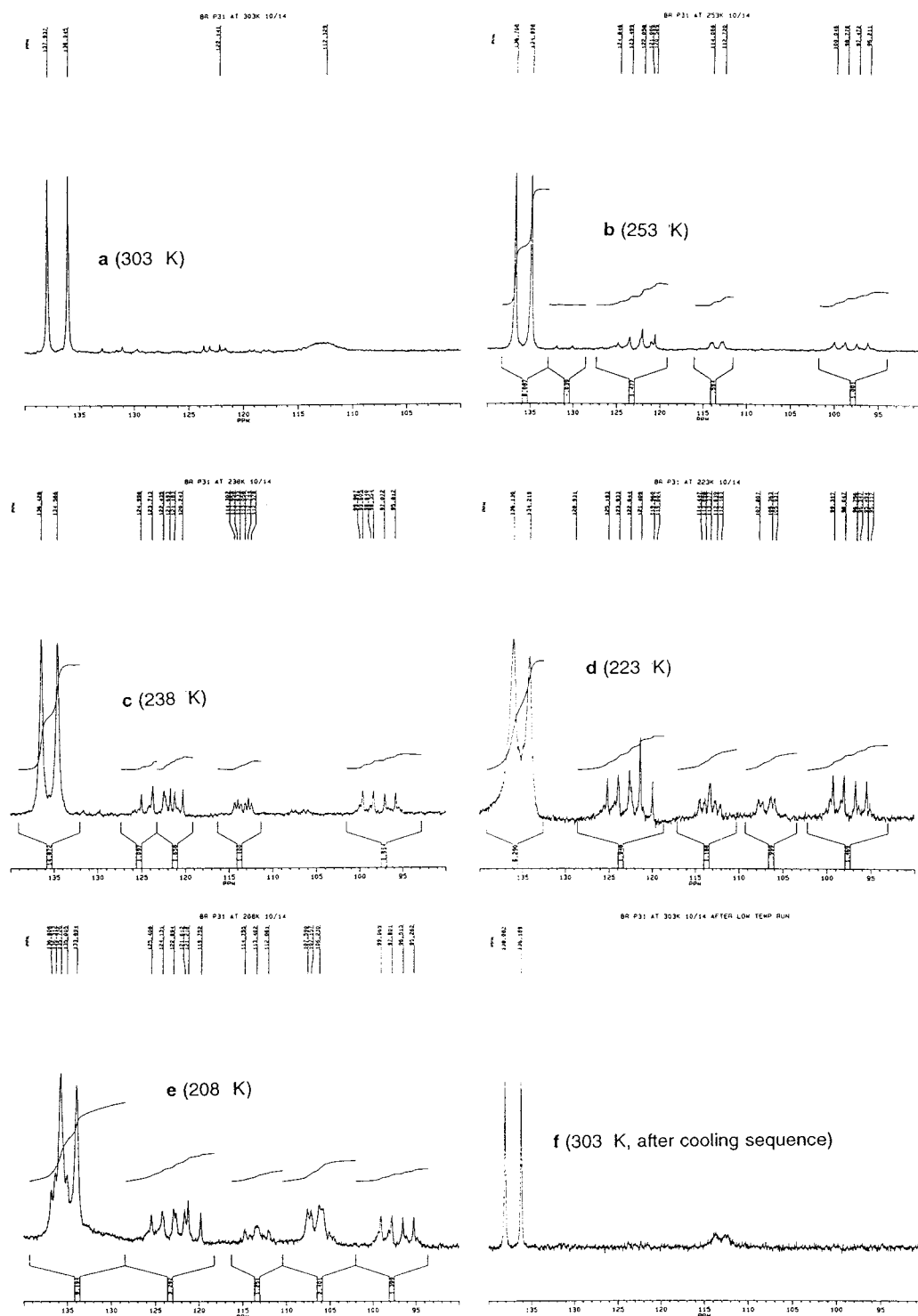


Figure 14. Temperature-dependent ^{31}P NMR spectra of diastereomers of $[\text{dimethyl itaconate}]\text{Rh}^+[\mathbf{7d}]$.

proportion of the unreacted solvate complex $[\text{CD}_3\text{OD}]_2\text{Rh}^+[\mathbf{7x}]$ still present in the case of the latter, even at 208 K (compare Figures 12e and 13e with Figures 14e and 15e). The relevance of these observations to the selectivity must await further studies.

Conclusions

Enantioselectivities of the Rh(I)-catalyzed hydrogenations of dimethyl itaconate and methyl α -*N*-acetylcinnamate using (1,2-diarylphosphinoxy)cyclohexane as

ligands are affected by substituents on the *P*-aryl groups. The electron-rich 3,5-dimethylphenyl substituent gives the highest ee, whereas the corresponding 3,5-bis-trifluoromethylphenyl derivative gives the lowest. The same substituent effects are seen with 2,3-diarylphosphinites derived from phenyl- β -D-glucopyranoside. In this work, we have tried to clarify these remarkable effects at two levels. First, we obtained crystal structures of a number of relevant precatalysts ($[\text{phosphinite}]_2\text{Rh}^+[\text{diolefin}]\text{X}^-$) and studied in detail their ground-state conformations. These conformations were compared among themselves

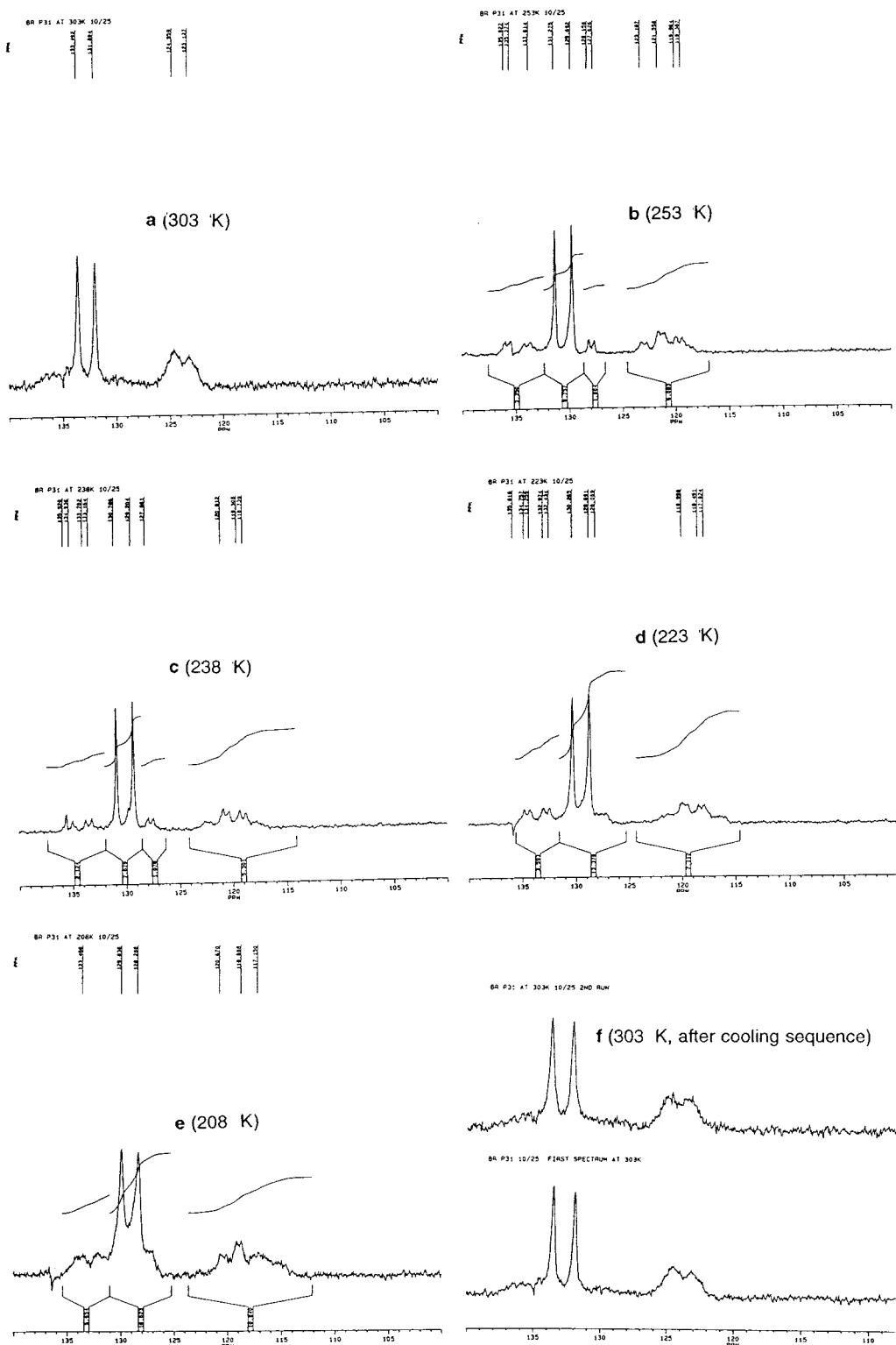


Figure 15. Temperature-dependent ^{31}P NMR spectra of diastereomers of $[\text{dimethyl itaconate}]\text{Rh}^+[\mathbf{7e}]$.

and with those of other related structures with the goal of testing whether electronic effects alone can alter the ground-state conformation of a precatalyst. The importance of such a study is underscored by the highly predictable empirical correlations that have evolved, which relate the ground-state conformations of the precatalyst ($[\text{phosphine}]\text{Rh}^+[\text{dioline}]$) to the sense of asymmetric induction. In the event, a study of six complexes with different phosphinites reveals that the gross conformational features of the precatalysts are largely

unaffected by electronic effects, which means that one has to look elsewhere (to the stability and/or reactivity of other intermediates along the reaction path) for an explanation of the electronic amplification. In the itaconate reduction, where the diastereomers of the $[\text{itaconate}]\text{Rh}^+[\text{phosphinite}]$ complex are detectable by ^{31}P NMR, there is a clear difference in the ratio of the major to minor diastereomer when the 3,5-dimethylphenylphosphinite (**7a**) is employed as the ligand, as compared to when the unsubstituted diphenylphosphinite **7b** is used.

We have not been able to establish the diastereomer ratio in the more electron-deficient 3,5-difluorophenyl (**7d**) and 3,5-bis-trifluoromethylphenyl (**7e**) systems. In the case of **7d**, the isomers could not be reliably identified. With **7e**, even at the coldest temperature (208 K) the isomers appear to be in fast equilibrium. Further insight into the diastereomer equilibria may be gained by looking at (^{31}P , ^{31}P)- $\{^1\text{H}\}$ -2D EXSY NMR of the exchanging system.^{4c} We plan to pursue these studies in the future.

Experimental Section

General Methods. Manipulations of air- and moisture-sensitive materials were conducted in a nitrogen atmosphere by using either Schlenk techniques or a Vacuum Atmospheres drybox. Tetrahydrofuran (THF), ether, dimethoxyethane (DME), hexane, and pentane were distilled from sodium benzophenone ketyl under nitrogen. Benzene and toluene were distilled from lithium aluminum hydride and stored over activated 4 Å molecular sieves. Methylene chloride, dimethylformamide (DMF), and acetonitrile were distilled from calcium hydride and stored over activated 3 Å, molecular sieves. Flash column chromatography was carried out on 230–400 mesh (0.040–0.063 mm) silica (EM Reagents). Gas chromatographic (GC) analysis was performed with a Hewlett-Packard (HP) model 5890 GC fitted with a HP3396A integrator. Conversions were determined using an HP cross-linked methyl silicone capillary column (30 m \times 0.530 mm). GC separations of the amino acid ester enantiomers were accomplished using Chirasil L-Val on WCOT fused silica (25 m \times 0.25 mm, 0.12 mm film thickness) capillary GC column purchased from Chrompack (1130 Route 202 South, Raritan, NJ 08869). The succinate products were separated on a Chiraldex GTA capillary column (10 m \times 0.25 mm) purchased from Bodman (P.O. Box 2421, Aston, PA 19014). HPLC separations were carried out on Chiralcel OJ or Chiralcel OB HPLC columns (25 cm \times 4.6 mm) manufactured by Daicel (available from Chiral Technologies, Inc., 730 Springdale Drive, Drawer 1, Exton, PA 19341). Preparation of the sugar-derived ligands, Rh-complexes, and the acetamidocinnamate substrates have been described before.^{6b}

Ligands and Catalysts from (1*S*,2*S*)-trans-1,2-Cyclohexanediol. (1*S*,2*S*)-bis-Diphenylphosphinocyclohexane (7b**).** This experiment was done inside the drybox. To 200 mg (1.72 mmol) of azeotropically dried (1*S*,2*S*)-trans-1,2-cyclohexanediol and 11 mg (0.05 equiv) of 4-(dimethylamino)pyridine dissolved in 2 mL of CH_2Cl_2 and 1 mL of pyridine was added, at 0 °C, 0.836 g (3.78 mmol) of chlorodiphenylphosphine in 3 mL of methylene chloride. An additional 1 mL of methylene chloride was used to facilitate transfer of the chlorophosphine quantitatively. The mixture was warmed to room temperature and was stirred for 18 h. The precipitated solids were filtered off with the aid of a cotton-plugged disposable pipet. The NMR spectrum of this solid showed that it was pyridine hydrochloride. The vials were washed with 2 mL of 1:1 ether/hexanes, and the solid in the disposable pipet was washed with this solvent. The filtrate was concentrated to get a white solid. The product was recrystallized from benzene (95% yield): ^1H NMR (C_6D_6) 0.70–0.95 (m, 2 H), 1.10–1.45 (m, 4 H), 1.90–2.05 (m, 2 H), 4.05 (m, 2 H), 6.70–7.15 (m, aromatic), 7.45–7.70 (m, aromatic); ^{31}P NMR 108.7.

[7b]Rh⁺(COD) SbF₆⁻. This complex was prepared by adding a CH_2Cl_2 solution of the bis-phosphinite to a solution of $(\text{COD})_2\text{Rh}^+ \text{SbF}_6^-$ in CH_2Cl_2 at room temperature and stirring the solution overnight. The low-boiling components were removed, and the NMR spectra were recorded in CDCl_3 : ^1H NMR δ 0.70–1.15 (m, 4 H), 1.35–1.60 (d, br, 2 H), 1.78 (d, br, 2 H), 2.10–2.30 (m, 4 H), 2.32–2.60 (m, 4 H), 3.82–4.02 (m, 2 H), 4.42 (m, br, 2 H), 4.90 (s, br, 2 H), 7.00–7.80 (m, aromatic); ^{31}P NMR (CDCl_3) δ 131.0 (d, $J_{\text{Rh-P}} = 177$). Minor peaks (together <2%) at δ 122.4 (dd $J = 173, 6$). The experiment was repeated in THF, and the ^{31}P spectrum was recorded in THF- d_6 : 129.7 (d, $J = 178$ Hz), no minor peaks were visible under these conditions. The experiment was

repeated in acetone and the spectrum was recorded in $\text{CD}_2\text{-Cl}_2$: ^{31}P NMR (CD_2Cl_2) 133.3 (d, $J = 179$ Hz). The other peak δ 122.4 (dd $J = 173, 6$ Hz) accounted for <9% area.

A sample of this compound was recrystallized from benzene by slow evaporation, and X-ray structure analysis was done to confirm the structure (see ref 6b for details).

[7b]Rh⁺(NBD)SbF₆⁻. The title compound was prepared by the above procedure, except that Rh^+ (norbornadiene)₂ SbF_6^- was substituted for $\text{Rh}(\text{COD})_2^+\text{SbF}_6^-$.

X-ray Crystallography. Crystal data: $\text{SbRhP}_2\text{F}_6\text{O}_2\text{C}_{37}\text{H}_{38}$, from benzene, red-orange, irregular block, $\sim 0.40 \times 0.30 \times 0.37$ mm, monoclinic, $C2$ (No. 5), $a = 38.889(4)$ Å, $b = 10.617(2)$ Å, $c = 19.134(4)$ Å, $\beta = 114.27(1)^\circ$, from 25 reflections, $T = -70$ °C, $V = 7201.9$ Å³, $Z = 8$, $\text{FW} = 915.32$, $D_c = 1.688$ g/cm³, $\mu(\text{Mo}) = 13.55$ cm⁻¹.

Data collection: Enraf-Nonius CAD4 diffractometer, Mo $K\alpha$ radiation, 7856 data collected, $2.3^\circ \leq 2\theta \leq 52.0^\circ$, maximum $h, k, l = 47, 13, 23$, data octants = +++, -+-, ω scan method, scan width = $1.20\text{--}1.50^\circ\omega$, scan speed = $1.50\text{--}6.70^\circ/\text{min}$, typical half-height peak width = $0.13^\circ\omega$, two standards collected 32 times, adjusted for a 6% decrease in intensity, 9.1% variation in azimuthal scan, no absorption correction, 226 duplicates, 1.7% R -merge, 5278 unique reflections with $I \geq 3.0\sigma(I)$.

Solution and Refinement. Solved by direct methods (SHELX). The asymmetric unit consists of two ion pairs in general positions related by a pseudomirror at (0, 0.47, -0.50). This results in near $C2/c$ space-group symmetry and high correlations in the refinement. Hydrogen atoms were included as fixed atoms in idealized positions. Both SbF_6^- anions show high thermal motion or disorder. The acentric space group indicates an optically pure enantiomer, here chosen to be C_{11}/S , C_{12}/S based on the lowest R value for anomalous terms (the centric positioning of the heavy atoms and the oscillation in the refinement limits the sensitivity of the anomalous dispersion test), refinement by full-matrix least-squares on F , scattering factors from *International Tables for X-ray Crystallography*, Vol IV, including anomalous terms for Sb, R , biweight $\propto [\sigma^2(1) + 0.0009(1)^2]^{-1/2}$ (excluded 1), refined anisotropic: Sb, Rh, P, F, isotropic: F, C, fixed atoms: H; 846 parameters, data/parameter ratio = 6.24, $R = 0.049$, $W = 0.048$, error of fit = 1.75, max $\Delta/\sigma = 1.32$. The disordered fluorine atoms of one SbF_6^- were modeled with two-half-weighted orientations, while the second SbF_6^- was modeled with normal anisotropic thermal tensors. Due to high correlations, several atoms could not be refined anisotropically (Table 1 in the Supporting Information). Refinement in $C2/c$ (with omission of ~ 150 reflections, resulted in $R = 0.082$, $R_w = 0.081$), largest residual density = 2.52 e/Å³. There are four intense residual peaks near two phenyl rings and midway between the PO_2C_2 bridge on each cation. These may result from refinement correlations or crystal imperfections.

Analysis confirms the structure of the complex as the SbF_6^- salt. Although the bidentate ligand is enantiomeric, the relative orientation of the phosphine phenyl rings results in two coordination modes creating a pseudoinversion center. Accurate assessment of bond parameters is limited by the disorder and the high least-squares correlations (highest correlation = 0.89).

Fractional coordinates, isotropic and anisotropic thermal parameters, and complete listing of bond angles and bond lengths are given in the Supporting Information.

X-ray Crystallography of [7b]Ni(Br)₂. This complex was prepared by dissolving 0.066 g (0.137 mmol) of $\text{NiBr}_2 \cdot \text{DME}^{5b}$ and 0.042 g (0.137 mmol) of **7b** in 3 mL of THF. The mixture was filtered, and to the filtrate were added DME and then hexane to induce crystallization.

Crystal data: $\text{Br}_2\text{NiP}_2\text{O}_2\text{C}_{30}\text{H}_{30}$, red, rod, from DME/hexane, $\sim 0.50 \times 0.10 \times 0.05$ mm, orthorhombic, $P2_12_12_1$ (No. 19), $a = 17.593(1)$ Å, $b = 34.680(2)$ Å, $c = 9.565(1)$ Å, $T = -75$ °C, $V = 5835.9$ Å³, $Z = 8$, $\text{FW} = 703.04$, $D_c = 1.600$ g/cm³, $\mu(\text{Mo}) = 35.14$ cm⁻¹.

Data collection: Rigaku RU300, R-AXIS image plate area detector, Mo $K\alpha$ radiation, filament size = 0.5 mm \times 1.0 cm, anode power = 55 kV \times 200 ma, crystal to plate distance =

79.1 mm, 210 μ pixel raster, number of frames = 45, oscillation range = 2.0°/frame, exposure = 2.0 min/frame, box sum integration, 11055 data collected, $2.3^\circ \leq 2\theta \leq 49.7^\circ$, maximum $h, k, l = 20, 40, 11$, corrected for absorption (DIFABS), range of transmission factors = 0.29–1.05, 2013 duplicates, 4.1% R -merge, 3583 unique reflections with $I \geq 3.0\sigma(I)$.

Solution and Refinement. Structure solved by automated Patterson analysis (PHASE). The asymmetric unit consists of two independent molecules in general positions. Hydrogen atoms were idealized with $C-H = 0.95 \text{ \AA}$. Refinement by full-matrix least squares on F , scattering factors from *International Tables for X-ray Crystallography*, Vol IV, including anomalous terms for Br, Ni, P, biweight $\propto [\sigma^2(l) + 0.0009(1)^2]^{-1/2}$ (excluded 4), refined anisotropic: Br, Ni, P, O; isotropic: C; fixed atoms: H; 662 parameters, data/parameter ratio = 5.41, $R = 0.063$, $R_w = 0.052$, error of fit = 1.27, max $\Delta/\sigma = 0.02$. [The acentric space group indicates an optically pure enantiomorph. The absolute configuration was determined from an R -value test ($R = 8.30$ and 7.79 vs 7.23 and 6.64)].

The analysis confirms the structure of the [7b]NiBr₂ complex. Fractional coordinates, isotropic and anisotropic thermal parameters, and a complete listing of bond angles and bond lengths are given in the Supporting Information.

Synthesis of Other Phosphinites and Their Rh-Complexes. The following diarylphosphinites and related complexes were prepared by similar routes:

(1*S*,2*S*)-1,2-[Bis-(3,5-dimethyl)phenylphosphinoxy]cyclohexane (7a): ¹H NMR (C₆D₆) δ 0.90 (m, 2 H), 1.30 (m, 2 H), 1.42 (m, 2 H), 1.85–2.05 (m, 2 H), 1.95 (s, 12 H), 2.00 (s, 12 H), 4.21 (m, 2 H) 6.60 (s, br, 2 H), 6.69 (s, br, 2 H), 7.38 (d, $J = 8 \text{ Hz}$, 2 H), 7.45 (d, $J = 8 \text{ Hz}$); ³¹P NMR δ 111.5 (s).

[7a]Rh⁺(COD) SbF₆⁻: ³¹P NMR(CD₂Cl₂) δ 133.4 (d, $J_{\text{RhP}} = 178 \text{ Hz}$).

(1*S*,2*S*)-1,2-[Bis-(3,5-difluoro)phenylphosphinoxy]cyclohexane (7d): ¹H NMR (C₆D₆) δ 0.65 (m, 2 H), 0.80–1.20 (m, 4 H), 1.55 (m, 2 H), 3.60 (m, 2 H), 6.25 (m, br, aromatic), 6.75 (m, br, aromatic), 6.85 (m, br, aromatic); ³¹P NMR (C₆D₆) δ 103.9.

[7d]Rh⁺(COD) OTf⁻. This complex was prepared by mixing an acetone solution of the ligand and Rh⁺(COD)₂OTf⁻ in stoichiometric proportions at room temperature: ¹H NMR inter alia δ 4.80 (s, br, 2 H), 5.05 (m, 2 H), 5.38 (m, 2 H); ³¹P NMR (CD₃COCD₃) δ 120.7 (d, $J_{\text{RhP}} = 183 \text{ Hz}$); ¹⁹F NMR (CD₃-COCD₃) δ -79.05 (s, 3 F), -107.8 (d, br, 8 F).

[7d]Rh⁺(COD)SbF₆⁻. To a solution of 227 mg (0.41 mmol) of Rh⁺(COD)₂SbF₆⁻ in 1 mL of acetone was added 270 mg (0.44 mmol) of the bis-phosphinite in 2 mL of acetone at room temperature. The mixture was stirred for 10 min, and 5 mL of CH₂Cl₂ was added followed by 20 mL of hexane. The precipitated solid was isolated and identified as the desired complex from its characteristic NMR spectra: ¹H NMR (CD₂-Cl₂) δ 1.00–1.45 (m, 4 H), 1.60 (m, 2 H), 1.90 (d, br, $J = 12 \text{ Hz}$, 2 H), 2.30–2.65 (m, 8 H), 4.15 (s, br, 2 H), 4.75 (m, 2 H), 5.08 (m, 2 H), 7.00–7.20 (m, aromatic); ³¹P NMR (CD₂Cl₂) δ 123.4 (d, $J_{\text{RhP}} = 183 \text{ Hz}$); (THF-*d*₆) δ 119.1 ($J_{\text{RhP}} = 178 \text{ Hz}$).

The chloride-bridged dimer ([7d]Rh(μ -Cl)₂) was prepared according to the procedure given below for 7e: (CD₂Cl₂) δ 131.5 (d, $J = 219 \text{ Hz}$).

(1*S*,2*S*)-[Bis-1,2-bis-(3,5-bis-trifluoromethyl)phenyl]phosphinoxy]cyclohexane (7e): ¹H NMR (C₆D₆) δ 0.50–0.70 (m, 2 H), 0.80–1.10 (m, 4 H), 1.35–1.50 (d, br, 2 H), 3.70 (m, 2 H), 7.42 (s, 2 H), 7.52 (s, 2 H), 7.75 (d, $J = 7 \text{ Hz}$, 4 H), 7.90 (d, $J = 7 \text{ Hz}$, 4 H); ¹⁹F NMR δ 101.9; ¹H NMR (CD₂Cl₂) δ 1.20–2.00 (4 sets of m, 8 H), 4.20 (m, 2 H), 7.60 (s, 2 H), 7.70 (d, $J = 5 \text{ Hz}$, 4 H), 7.81 (s, 2 H), 7.87 (d, $J = 7 \text{ Hz}$, 4 H); ³¹P NMR (CD₂Cl₂) δ 102.3; ³¹P (THF-*d*₆) δ 99.64. Anal. Calcd for C₃₈H₂₂O₂P₂F₂₄: C, 44.38; H, 2.16. Found: C, 44.37; H, 2.53.

Preparation of Chloride-Bridged Dimer [7e]Rh(μ -Cl)₂. To a solution of 13 mg (0.02 mmol) of chloro-bis-(cycloocten- ϵ)rhodium(1) dimer in \sim 1 mL of CD₂Cl₂ was added 44 mg (0.04 mmol) of the bis-phosphinite in \sim 1 mL of CD₂Cl₂, and the mixture was stirred for 30 min at room temperature. The solvent and excess cyclooctene were pumped off, and ³¹P NMR was recorded in CD₂Cl₂. A major doublet, presumably due to the bridged dimer, appeared at δ 130.17 (d, $J = 218 \text{ Hz}$).

The same experiment done in acetone-*d*₆ gave the following peaks (inter alia): ³¹P (acetone-*d*₆) δ 127.67 (d, $J = 218 \text{ Hz}$).

The experiment was repeated as follows in a different procedure. To a solution of 103 mg (0.10 mmol) of the diphosphinite 7e in 10 mL of benzene was added chloro(1,5-cyclooctadiene)rhodium(1) dimer (30 mg, 0.6 mmol), and the mixture was brought to reflux. To this solution was added 35 mg (0.10 mmol) of silver hexafluoroantimonate, and the solution was filtered while hot. Concentration and reprecipitation yielded a solid whose ³¹P NMR (CD₂Cl₂) (δ 129.4, d, $J = 217 \text{ Hz}$), and the corresponding minor peaks looked remarkably like the one from previous experiment with the major product as the chloride-bridged dimer.

Reaction of [7e] with Rh⁺(COD)₂SbF₆⁻. To a solution of 56 mg of Rh⁺(COD)₂SbF₆⁻ in 1 mL of acetone, was added 103 mg (0.1 mmol) of the bis-phosphinite in 2 mL of acetone and the mixture was stirred for 3 h. The reaction mixture was concentrated, and excess hexane was added. The precipitated salt was collected and analyzed. ³¹P NMR in CD₂Cl₂ was exceptionally clean in ³¹P NMR δ 129.30 (d, $J = 216$). The major compound was identified as the bridged complex prepared by the independent routes described above. A single crystal obtained from the NMR solution by slow evaporation was subjected to X-ray analysis, and the Cl-bridged structure was confirmed.

A minor component (\sim 6%) whose ³¹P signal appeared at δ 124.8 ($J_{\text{RhP}} = 178 \text{ Hz}$) was identified as the cationic complex [7e]Rh⁺[COD]SbF₆⁻ by comparison of spectral data, especially the $J_{\text{Rh-P}}$ coupling constant, with those of a complex made in a chloride-free medium (see below).

Repetition of the reaction in CH₂Cl₂ gave essentially the same compound as the major product: ³¹P NMR (CD₂Cl₂) δ 129.4 (d, $J_{\text{Rh-P}} = 217 \text{ Hz}$) + other peaks; ³¹P NMR (CDCl₃) δ 119.6 ($J_{\text{Rh-P}} = 178 \text{ Hz}$) (cationic complex?); 125.2 ($J_{\text{Rh-P}} = 230 \text{ Hz}$) (dimer?).

The component showing δ 119.6 is relatively insoluble in benzene, supporting the cationic nature.

When the reaction is carried out in CH₂ClCH₂Cl as the solvent only the cationic complex was obtained, presumably because ClCH₂CH₂Cl is a poor Cl⁻ donor, and when the spectrum was run in THF-*d*₆, the following clean spectrum was observed: ³¹P NMR (THF-*d*₆) δ 129.17 (d, $J_{\text{Rh-P}} = 193 \text{ Hz}$).

It is believed that the highly electrophilic Rh complex abstracted the Cl from the methylene chloride solvent in the above experiments.

X-ray Crystallography of Chloride-Bridged Dimer ([7e]Rh(μ -Cl)₂). **Crystal data:** Rh₂Cl₃P₄F₄₈O₄C₇₇H₄₇, from CH₂Cl₂, gold, plate, \sim 0.51 \times 0.20 \times 0.45 mm, monoclinic, $P2_1$ (No. 4), $a = 14.576(4) \text{ \AA}$, $b = 21.770(10) \text{ \AA}$, $c = 15.185(4) \text{ \AA}$, $\beta = 108.16(1)^\circ$, $T = -70^\circ \text{ C}$, $V = 4578.5 \text{ \AA}^3$, $Z = 2$, $FW = 2378.29$, $D_c = 1.725 \text{ g/cm}^3$, $\mu(\text{Mo}) = 6.52 \text{ cm}^{-1}$.

Data collection: Enraf-Nonius CAD4 diffractometer, Mo K α radiation, 10613 data collected, $1.9^\circ \leq 2\theta \leq 54.0^\circ$, maximum $h, k, l = 18, 27, 19$, data octants = +++, --+, ω scan method, scan width = 1.20–2.20° ω , scan speed = 1.50–5.00°/min, typical half-height peak width = 0.14° ω , two standards collected 49 times, adjusted for a 5% decrease in intensity (251 omitted), 9.6% variation in azimuthal scan, no absorption correction, 375 duplicates, 1.8% R -merge, 6855 unique reflections with $I \geq 3.0\sigma(I)$.

Solution and Refinement. Structure solved by automated Patterson analysis (PHASE). The asymmetric unit consists of one dimer and a partially occupied methylene chloride solvate. Hydrogen atoms were idealized with $C-H = 0.95 \text{ \AA}$, refinement by full-matrix least squares on F , scattering factors from *International Tables for X-ray Crystallography*, Vol. IV, including anomalous terms for Rh, Cl, biweight $\propto [\sigma^2(l) + 0.00091^2]^{-1/2}$, (excluded 13), refined anisotropic: Rh, Cl, P, F, O, C, isotropic: C, fixed atoms: H; 1246 parameters, data/parameter ratio = 5.49; final $R = 0.053$, $R_w = 0.047$, error of fit = 1.50, max $\Delta/\sigma = 1.32$. The multiplicity of the solvate molecule was adjusted to give a reasonable thermal parameter. No attempt was made to model the disordered CF₃ groups. Atom C47' was refined isotropically due to nonpositive thermal matrix, largest residual density = 0.70 e/Å³, near Cl3.

The analysis confirms the dimeric structure as a CH_2Cl_2 solvate. It is a neutral dimer with no cyclooctadiene. Fractional coordinates, isotropic and anisotropic thermal parameters, and a complete listing of bond angles and bond lengths are given in the Supporting Information.

Preparation of Bis-(pentafluorophenyl)chlorophosphine. Pentafluorobromobenzene (8.20 mL, 66.0 mmol) in dry THF (15 mL) was added dropwise to freshly crushed magnesium turnings (24.31 g, 69.0 mmol) in THF (60 mL). After 2 h, this solution was added slowly to a solution of $(^i\text{Pr}_2\text{N})\text{PCl}_2$ (5.76 g, 30.0 mmol) in THF (20 mL) at room temperature. The reaction mixture was heated to reflux. After 13 h, the mixture was cooled to room temperature, and saturated aqueous $\text{NH}_4\text{-Cl}$ (80 mL) was added. The aqueous layer was extracted with hexane (80 mL \times 3), and the combined organic extract was dried (Na_2SO_4) and concentrated in vacuo to give $(\text{C}_6\text{F}_5)_2\text{PN}(i\text{-Pr})$ as a colorless oil. Crystallization with methanol gave white crystals (11.1 g, 79.8%): mp = 79–82 °C; $^1\text{H NMR}$ (CDCl_3) δ 3.58 (m, 1H), 1.19 (d, J = 6.1 Hz, 6 H); $^{31}\text{P NMR}$ (CDCl_3) δ 1.61 (quintet, J = 29.8 Hz).

Dry HCl was passed through a solution of the aminophosphine (2.45 g, 5.29 mmol) in dry cyclohexane (40 mL) at room temperature for 20 min. After filtration under argon atmosphere and concentration, 1.97 g (93.1%) of $(\text{C}_6\text{F}_5)_2\text{PCl}$ was collected as a colorless oil: ^{31}P (CDCl_3) δ 35.37 (quintet, J = 38.5 Hz) (lit.³⁸ δ 37.1 (CH_2Cl_2)).

Preparation of (1*R*,2*R*)-1,2-bis-[(dipentafluorophenyl)phosphinoxy]cyclohexane: $^1\text{H NMR}$ (CDCl_3) δ 3.99 (m, 2 H), 2.07 (m, 2 H), 1.73–1.43 (m, 4 H), 1.27 (m, 2 H); $^{31}\text{P NMR}$ (CDCl_3) δ 84.95 (quintet, J = 41.2 Hz).

Preparation of [(1*R*,2*R*)-1,2-Bis-(dipentafluorophenyl)phosphinoxy]cyclohexane[Rh⁺(COD)SbF₆⁻]. (1*R*,2*R*)-1,2-Bis-(dipentafluorophenyl)phosphinoxycyclohexane (0.17 g, 0.20 mmol) in dichloroethane (1 mL) was added slowly to a solution of $\text{Rh}^+(\text{COD})_2\text{SbF}_6^-$ (0.11 g, 0.20 mmol) in dichloroethane (1 mL) at room temperature. After 30 min, the reaction mixture was concentrated to give the product as an orange solid: $^1\text{H NMR}$ (CD_2Cl_2) 5.76 (s, br, 2 H), 4.94 (s, br, 2 H), 4.56 (q, J = 7 Hz, 2 H), 3.63 (s, br, 2 H), 2.63–2.17 (m, 6 H), 0.91–1.83 (m, 8 H); $^{31}\text{P NMR}$ (CD_2Cl_2) 104.96 (d, J = 201 Hz).

[Note that this complex has the 1*R*,2*R* configuration. In Table 4, appropriate changes in the absolute configuration of the products obtained using this ligand have been made to account for this.]

Preparation of Unsymmetrical Phosphinites. (1*S*,2*S*)-[1-diphenylphosphinoxy-2-bis-(3,5-bis-trifluoromethylphenyl)phosphinoxy]cyclohexane (7h). The following procedure was performed inside a drybox. A solution of 58 mg (0.50 mmol) of the diol and 5 mg of DMAP in 2 mL of 1:1 CH_2Cl_2 and pyridine was chilled inside a freezer at –33 °C, and to this was added, over 5 min, a CH_2Cl_2 solution of 232 mg (0.48 mmol) of bis-(3,5-bis-trifluoromethylphenyl)chlorophosphine. The mixture was allowed to warm to room temperature. After 3 h, the low-boiling solvents were removed on a high vacuum pump. To the residue was added 1.5 mL of benzene, and the precipitated solids were removed by filtration through a cotton pad in a small disposable pipette. The benzene solution was concentrated, and the product was chromatographed on silica gel (dried at 200 °C and cooled under nitrogen) inside a drybox using 10–15% ether/cyclohexane as the solvent. The fastest moving band was collected and was identified as **7e** by NMR. The major product (190 mg, 66%) was identified as the monophosphinite from the following data: $^1\text{H NMR}$ (C_6D_6) δ 0.80–1.80 (m), 3.01 (m, 1 H), 3.20 (m, 1 H), 7.57 (d, J = 8 Hz, 2 H), 7.86 (d, J = 5 Hz, 2 H), 8.02 (d, J = 5 Hz, 2 H); $^{31}\text{P NMR}$ δ 100.8.

The product from the previous reaction (190 mg, 0.35 mmol) was dissolved in 1 mL of CH_2Cl_2 and 1 mL of pyridine, and 3 mg of 4-(dimethylamino)pyridine was added. To this solution was added a CH_2Cl_2 solution of 72 mg (0.33 mmol) of diphenylchlorophosphine at ~0 °C. The reaction was allowed to warm to room temperature. After 16 h, the mixture was concentrated

on a vacuum pump. To the residue was added 1 mL of benzene, and the precipitated solids were removed by filtration through a cotton plug. Column chromatography inside the drybox using 10% ether/cyclohexane as the solvent gave pure **7h**: $^1\text{H NMR}$ (C_6D_6) δ 0.70 (m, br, 2 H), 1.00–1.20 (m, br, 4 H), 1.55 (d, br, J = 12 Hz, 1 H), 1.75 (d, J = 12 Hz, 1 H), 3.85 (s, br, 2 H), 6.75–7.10 (m), 7.25 (m), 7.35–7.60 (m), 7.80–7.90 (q, J = 4 Hz), (6.75–7.90 all aromatic); $^{31}\text{P NMR}$ δ 99.5 (s, 1 P), 109.4 (s, 1 P). Two other minor peaks at δ 100.9 and 107.7 (together 4% signal intensity) have been tentatively identified as due to the two symmetrical phosphinites formed by an exchange reaction.

[(1*S*,2*S*)-[1-Diphenylphosphinoxy-2-bis-(3,5-bis-trifluoromethylphenyl)phosphinoxy]cyclohexane][Rh⁺(COD)SbF₆⁻]. This complex was made in acetone by mixing stoichiometric amounts of the reagents: $^{31}\text{P NMR}$ (CD_3COCD_3) δ 125.5 (dd, J_{PRh} = 268 Hz, J_{PP} = 36 Hz, 1 P), 126.8 (dd, J_{PRh} = 243 Hz, J_{PP} = 36 Hz, 1 P).

[(1*S*,2*S*)-[1-Diphenylphosphinoxy-2-bis-(3,5-bis-trifluoromethylphenyl)phosphinoxy]cyclohexane][Rh⁺(COD)OTf⁻]. This complex was prepared in DME: $^{31}\text{P NMR}$ (CD_3COCD_3) δ 124.8 (dd, J_{PRh} = 195 Hz, J_{PP} = 36 Hz, 1 P), 126.6 (dd, J_{PRh} = 170 Hz, J_{PP} = 36 Hz, 1 P).

[(1*R*,2*R*)-[1-Bis(pentafluorophenyl)phosphinoxy-2-bis-(3,5-dimethylphenyl)phosphinoxy]cyclohexane][Rh⁺(COD)SbF₆⁻ (7g): $^{31}\text{P NMR}$ (CD_2Cl_2) δ 133.28 (dd, 1 P, J_{PRh} = 168 Hz, J_{PP} = 28 Hz), 102.00 (dq, 1 P, J_{PRh} = 211 Hz, J_{PP} = 28 Hz).

[Note that this complex has the (1*R*,2*R*) configuration. In Table 4, appropriate changes in the absolute configuration of the product have been made to account for this.]

Typical Scouting Procedure for Hydrogenation of Acetamidoacrylate Derivatives (Eq 2). In the drybox, a 150 mL Fisher-Porter tube was loaded with 50 mg (0.23 mmol) of acetamidoacrylate derivative, 1 mg (0.4 mol %) of **3b**, and 2 mL of THF. After sealing, the tube was removed from the drybox and placed behind proper shielding. With adequate stirring of the solution at room temperature, the tube was charged with 40 psi of H₂ gas and vented. This procedure was repeated twice more. The tube was charged with 30–40 psi of H₂. After 3 h, the tube was vented. The conversion as estimated by gas chromatography was quantitative in most instances. When a methyl ester derivative of **1** was used, the crude mixture was analyzed directly by GLPC (Chirasil S-Val, 170 °C/20 min, programmed for 10 °C/min to 195 °C, 195 °C/30 min. See ref 6b for retention times of the two enantiomers.

Typical Scouting Procedure for Rh-Catalyzed Hydrogenation of Dimethyl Itaconate. Dimethyl itaconate (0.12 g, 0.77 mmol) was dissolved in 3 mL of THF and placed in a Fisher-Porter apparatus in a drybox. The cationic Rh catalyst (typically 0.01 mmol) dissolved in 2 mL of THF was added to the itaconate solution. The apparatus was taken outside the drybox, and the reaction was placed under 45 psi of hydrogen after three evacuation–refill cycles as described above. The reaction was allowed to stir overnight, and it was analyzed by GC. The reaction was exceptionally clean and the yield nearly quantitative. On a Chiraldex GTA column (initial temperature 85 °C, initial time 20 min, rate of heating 5 °C/min, final temperature 95 °C), the (*S*) isomer of the product appears at 6.30 min and the (*R*)-isomer at 6.60 min. Each reaction was repeated twice, and the ee's are recorded in Table 3. Absolute configurations of the product enantiomers were determined by comparison of GC retention times with those of authentic materials obtained from a known hydrogenation catalytic, (2*S*,4*S*)-[BPPM]Rh⁺(COD)SbF₆⁻.¹⁵

A Typical Preparation of [Dimethyl itaconate]Rh⁺-[bis-diarylphosphinite]SbF₆⁻. The complex [(7a)Rh⁺(COD)]SbF₆⁻ (0.045 g, 0.043 mmol) was dissolved in 2 mL of CD_3OD in a 150 mL Fischer-Porter tube. The solution was hydrogenated at 45 psi of hydrogen until it turned brown-green. Subsequently, the Fisher-Porter tube was transferred back into the drybox, the gas was vented, and to the reaction mixture was added 0.040 g (0.25 mmol, 5.8 equiv) of dimethyl itaconate. The mixture was carefully transferred into an NMR tube and sealed, and the temperature-dependent $^{31}\text{P NMR}$ spectra were recorded at the various temperatures shown in Figure 13. At

the end of the low-temperature runs, the solution was brought back to room temperature and the spectrum was recorded. Thus, we have confirmed that all changes are reversible.

Acknowledgment. We are grateful to the National Science Foundation (CHE-9706766) and EPA/NSF Program for Technology for Sustainable Environment (EPA R826120-01-0) for financial support of this work. Further assistance by the Petroleum Research Fund (ACS) is also acknowledged. We thank Dr. Judy Galluci (OSU)

for her help in obtaining X-ray data from Cambridge Crystal Data Files. Dr. Charles Cottrell (OSU) helped with the low-temperature NMR studies.

Supporting Information Available: Tables of crystal data, structure solution and refinement, atomic coordinates, bond lengths and angles, and anisotropic thermal parameters for **12**, **14**, **15**, and **16**. This material is available free of charge via the Internet at <http://pubs.acs.org>.

JO9901182